MONTHLY WEATHER REVIEW

VOLUME 78 NUMBER 11

NOVEMBER 1950

CONTENTS

U. S. DEPARTMENT OF COMMERCE · WEATHER BUREAU

DEPARTMENT OF COMMERCE
CHARLES SAWYER, Secretary

WEATHER BUREAU
F. W. REICHELDERFER, Chief

MONTHLY WEATHER REVIEW

Editor, JAMES E. CASKEY, Jr.

Volume 78
Number 11

NOVEMBER 1950

Closed Jan. 15, 1951
Issued Feb. 15, 1951

VERTICAL STRUCTURE OF A MATURE TYPHOON

H. ARAKAWA

Meteorological Research Institute, Suginami-ku, Tokyo

[Original manuscript received September 13, 1950; revised manuscript received November 24, 1950]

ABSTRACT

Aerological observations made in a mature typhoon on August 31 and September 1, 1949, by the Central Meteorological Observatory, Tokyo, are given and time cross sections are constructed showing the distribution of temperature, potential temperature, pressure, and circulation acceleration. The vertical structure of the typhoon is discussed and the results compared with those previously given by Palmén and by Simpson.

The *Kitty** typhoon of August 27–September 2, 1949, was of great intensity, and the most destructive storm to visit Tokyo in recent years. Over 100 lives were lost as a result of the storm, and estimates of property damage run well over ¥ 15,000,000,000 (about $40,000,000).

On the night of August 31, approaching Tokyo from the south at the speed of about 50 km./hr., the storm center crossed the Kanto district about 30 to 50 km. west of the Central Meteorological Observatory (CMO). Table 1 shows the central pressure, the track, and the velocity of movement of the *Kitty* typhoon, and table 2 the records of meteorological conditions at Tokyo (CMO) during its passage.

Observation of the *Kitty* typhoon was distinguished by at least the following two interesting features: (a) The storm center crossed the land a short distance west of Tokyo, where the net of meteorological observations is fairly dense. (b) It is fortunate that a good number of radiosonde and wind observations were successfully obtained from the storm area. A number of regular and special radiosonde releases were made at stations (CMO, Haneda Weather Central, and Aerological Observatory at Tateno) under the influence of this typhoon. Radiosonde flights and rawin observations for the *Kitty* typhoon made by the staff of CMO are given in tables 3 and 4. These observations, which include a radiosonde flight made at Tokyo near the core of the typhoon shortly in advance of the center, have made it possible to construct a more complete picture of the vertical structure of a typhoon in a *mature* stage of development than has been possible before.

*Name given the typhoon for purpose of identification in advisories.

TABLE 1.—*Track, central pressure and movement of the Kitty typhoon Aug. 28–Sept. 1, 1949*

Date and hour (135th meridian civil time)	Central pressure (estimated) mb.	Locus of center		Movement of center	
		Latitude °N	Longitude °E	Direction	Speed km/hr
Aug. 28, 09h	980	23.2	154.5	NW	20
15	980	24.2	153.7	NW	20
21	980	25.0	152.8	NW	25
Aug. 29, 03h	980	25.8	151.8	NW	25
09	980	26.7	150.7	WNW	25
15	980	27.3	149.4	WNW	25
21	980	27.8	148.0	WNW	25
Aug. 30, 03h	980	28.4	146.5	WNW	25
09	980	29.0	145.1	WNW	25
15	970	29.6	143.6	WNW-NW	28
21	970	30.3	142.2	NW	28
Aug. 31, 00h	960	30.8	141.7	NW	30
03	960	31.5	141.0	NW	30
06	960	32.2	140.3	NW	30
09	950	32.7	139.9	NW	30
12	950	33.5	139.5	NW	25
13	950	33.6	139.4	NW	25
14	950	33.8	139.2	NW	25
15	950	34.1	139.0	NW-NNW	25
16	950	34.3	138.9	N	20
17	950	34.4	139.0	NNE	25
18	955	34.7	139.2	N	40
19	960	35.2	139.2	N	55
20	965	35.7	139.2	N	55
21	975	36.2	139.1	N	55
22	975	36.6	139.0	NNW	55
23	980	37.2	138.6	NNW	55
Sept. 1, 00h	980	37.6	138.4	N	50
01	980	37.9	138.5	N-NNE	50
03	980	38.8	138.7	NNE	50
06	980	40.3	139.0	NNE	50
09	985	41.5	140.0	NNE	50

Many papers concerning the vertical structure of the *Kitty* typhoon have been published under several titles [1, 2, 3, 4]. The following note attempts to summarize the salient features of the storm, obtained from all available sources of information, as a possible contribution to future studies of typhoon structure and to compare them with the picture of the vertical structure of tropical cyclones as previously given by Palmén [5], and Simpson [6].

TABLE 2.—*Meteorological observations at Tokyo (CMO), Aug. 31–Sept. 1, 1949*

Date and hour (135th meridian civil time)	Pressure (sea level) mb.	Temp. °C.	Humidity %	Wind direction	Wind speed m/sec.
Aug. 30, 24h	1011.5	25.0	94	NE	3.6
Aug. 31, 01h	1010.7	25.1	94	NE	3.4
02	1010.0	25.1	93	NE	4.4
03	1009.2	25.1	92	NE	3.4
04	1008.8	24.9	93	NE	4.4
05	1008.3	25.0	92	NE	5.4
06	1007.8	25.0	94	NE	5.5
07	1007.1	25.9	90	NE	7.6
08	1006.3	26.5	87	ENE	7.1
09	1005.2	26.6	86	ENE	8.2
10	1004.3	26.7	89	ENE	9.6
11	1002.8	27.5	81	ENE	10.1
12	1001.2	26.5	87	NE	11.5
13	999.9	26.1	88	E	12.7
14	997.8	25.9	90	E	13.7
15	996.8	25.7	90	E	14.2
16	995.0	25.6	90	ESE	18.0
17	993.0	25.7	89	ESE	17.1
18	989.5	25.4	88	E	17.6
19	986.4	24.9	86	ESE	20.2
20	986.6	24.2	91	E	19.4
21	988.7	23.6	95	SSE	22.2
22	991.6	23.5	96	S	21.6
23	994.4	24.4	93	S	22.8
24	998.0	24.7	93	S	15.5
Sept. 1, 01h	999.6	25.1	90	S	15.8
02	1002.2	25.6	88	S	12.4
03	1003.2	25.2	89	S	13.7
04	1003.8	25.5	88	S	11.7
05	1004.8	25.8	88	S	10.3
06	1005.9	25.3	88	S	9.1
07	1006.7	25.1	92	S	7.1
08	1007.5	25.2	91	S	8.5
09	1008.0	25.9	89	S	7.4
10	1008.6	26.3	88	SSE	7.6
11	1008.6	26.7	84	SSE	8.9
12	1008.6	27.5	78	SSE	8.5
13	1008.6	28.3	74	SSE	8.2
14	1008.4	27.5	79	SSE	9.4
15	1008.8	26.3	84	SSE	8.7
16	1009.0	26.1	86	SSE	6.5
17	1008.8	26.0	85	SSE	8.7
18	1009.8	25.6	88	SSE	7.4
19	1010.6	25.6	90	SSE	7.4
20	1011.1	25.3	90	SSE	3.6
21	1011.5	25.0	90	S	5.7
22	1011.6	24.6	91	S	5.9
23	1011.4	24.5	90	S	4.2
24	1011.3	24.3	90	S	3.6

Figure 1 is the time cross section showing the distribution of temperature (broken lines) and potential temperature (solid lines). It would appear that the core of the storm is decidedly warmer, especially at higher levels, than the air columns at 200 km. in the front and 300 km. in the rear from the center. And it would also appear that the core of the storm is decidedly higher in potential temperature, especially at higher levels. These two features are quite similar to Palmén's cross section [5], which shows that there is a marked descending motion in the free atmosphere in the core of the storm. It would appear that the storm region in the front and the rear of the core is decidedly colder both in air temperature and potential temperature, especially at higher levels, than the air columns at great distance from the center. The very heavy lines with considerable slope show the boundary surfaces separating two regions of ascending and descending air currents. This is quite *different* from Palmén's cross section. In the stormy region of any tropical storm in a mature stage of development there *must* be an intense ascending motion, which results in dynamical cooling and the uprush of the isentropic surface. So the vertical structure given for the *Kitty* typhoon seems to be more natural as well as more trustworthy than Palmén's cross section for the Miami-New Orleans hurricane of September 17–21, 1947.

If we suppose that the time cross section of the *Kitty* typhoon takes over the role of the *spatial* meridional cross section of the *Kitty* typhoon, we can reach some important conclusions. In view of the importance of baroclinicy

TABLE 3.—*Radiosonde observations by the Central Meteorological Observatory, Aug. 30–Sept. 1, 1949*

Release date and hour (135th meridian civil time)	Aug. 30, 1230			Aug. 31, 0904			Aug. 31, 1220			Aug. 31, 1330			Aug. 31, 1554			Aug. 31, 1849			Sept. 1, 0150			Sept. 1, 1100		
Height km.	Pressure mb.	Temperature °C.	Humidity %	Pressure mb.	Temperature °C.	Humidity %	Pressure mb.	Temperature °C.	Humidity %	Pressure mb.	Temperature °C.	Humidity %	Pressure mb.	Temperature °C.	Humidity %	Pressure mb.	Temperature °C.	Humidity %	Pressure mb.	Temperature °C.	Humidity %	Pressure mb.	Temperature °C.	Humidity %
0.5	957	25.7	59	953	22.8	91	948	22.4	96	948	23.3	94	944	23.1	92	935	22.1	90	947	22.8	93	955	23.1	97
1.0	904	21.4	68	899	20.5	87	895	20.8	96	895	20.7	97	891	20.7	92	881	18.8	94	893	20.5	87	901	20.4	87
1.5	853	18.6	71	848	18.4	86	844	17.4	96	844	18.0	98	840	17.8	92	832	16.2	97	843	17.6	86	849	18.3	75
2.0	804	16.7	66	803	16.0	84	796	15.8	96	796	15.9	98	792	15.2	90	784	14.4	92	795	16.4	79	801	16.9	73
3.0	715	13.0	53	711	11.5	77	707	10.5	96	707	10.5	99	704	10.8	86	696	10.6	89	705	12.7	63	712	13.1	65
4.0	633	7.4	37	629	7.2	76	627	6.2	96	627	7.7	100	623	5.5	86	616	6.1	81	625	5.5	75	632	6.5	74
5.0	560	1.6	29	556	1.8	70	553	0.1	96	555	2.8	100	551	0.9	86	545	1.5	88	552	−1.1	88	559	1.9	86
6.0	495	−3.5	25	491	−3.1	50							485	−4.6	85	481	−2.9	88	487	−5.0	91	493	−2.5	65
7.0	435	−9.1	21	432	−7.8	42							427	−10.9	77	424	−7.3	80	428	−9.4	88	433	−8.5	70
8.0	383	−14.6	20	380	−13.5	42							375	−14.9	69	372	−12.4	80	376	−13.5	86	381	−12.7	70
9.0	335	−21.1	20	332	−18.4	42							327	−21.4	68	325	−17.0	79	329	−19.2	85	333	−19.8	70
10.0	292	−29.3	18	289	−23.4	39							285	−28.2		285	−23.6	74	287	−26.2	83	291	−27.7	
11.0	253	−35.1		252	−29.3	38							248	−36.3		248	−28.7		249	−33.5		253	−33.9	
12.0	219	−41.8		219	−35.3								213	−43.3		216	−36.1		217	−42.0		219	−39.5	
13.0	188	−49.6		189	−44.2								184	−50.4		185	−42.7		187	−48.3		188	−44.1	
14.0	161	−58.6		163	−50.2								157	−58.0		159	−50.3		160	−56.8		163	−48.7	
15.0	137	−65.0		139	−59.3								135	−65.5		136	−56.4		136	−62.5		139	−53.4	
16.0				119	−66.0								112	−72.9		116	−63.9		115	−69.3		119	−59.3	
17.0				100	−66.8								96	−77.2		97	−69.0					101	−62.9	
18.0				85	−65.3								84	−73.0		83	−69.8					85	−62.2	
19.0				72	−63.4								68	−71.2		69	−70.0					73	−61.5	
20.0				61	−59.8																	63	−58.0	
21.0				52	−54.7																	53	−54.7	
22.0				45	−49.7																	45	−52.6	
Maximum height (m.)	15,479			24,697			5,019			5,587			19,097			19,377			16,902			22,036		
Remarks																The release was made shortly in advance of the core								

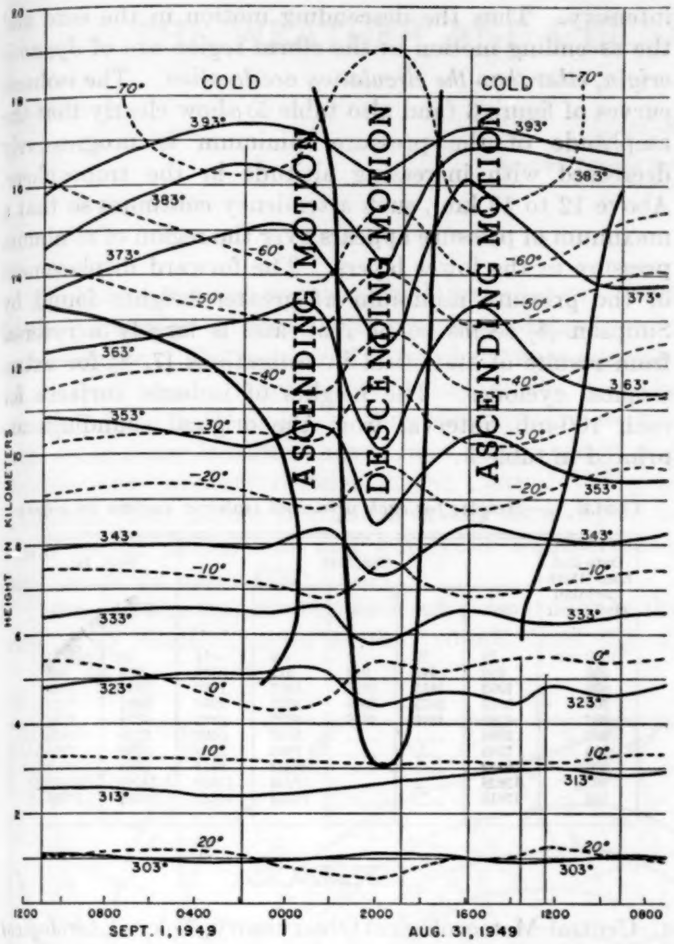

FIGURE 1.—Time cross section of the *Kitty* typhoon showing temperature (° C.) (broken lines) and potential temperature (° A.) (solid lines). The heavy solid lines with considerable slope separate two regions of ascending and descending air currents.

for the dynamics of a typhoon, the present author intends to evaluate the variation of the circulation with time, $\frac{dC}{dt}=-\oint\frac{dp}{\rho}$, where ρ is the density, p the atmospheric pressure. If the circulation in a vertical plane is to be computed, a convenient path of integration would consist of two isobars and two vertical lines connecting these isobars. In order to compute the intensity of the circulation acceleration in the cross section of the *Kitty* typhoon, one might choose the principal isobars p_1 and p_{1-100} and the verticals a_s and a_{s+1} connecting these isobars at two successive soundings (fig. 2). Integration along the isobars gives zero. From the hydrostatic equation, it follows that $-\frac{dp}{\rho}=gdz=d\psi$, where g is the acceleration of gravity, z the height, and ψ the geopotential. Thus, along the curves a_s and a_{s+1} the height differences between two successive principal isobars may be integrated so that $\frac{dC}{dt}=\psi_s-\psi_{s+1}$. The circulation acceleration is directed as indicated by the arrows in figure 2. Thus the circulation is upward toward lower pressure on the warmer side, downward toward higher pressure on the colder side, and from the colder to the warmer side along the higher pressure surface, and back from the warmer to the colder side along the lower pressure surface.

To evaluate the circulation acceleration, the isobars for every 100 mb. and the lines indicating the release time may be drawn in the cross section of the *Kitty* typhoon. The evaluated height differences are tabulated in figure 3, where the circulation acceleration in the direction indicated by the arrows in figure 2 is taken to be positive. The circulation accelerations are written for

TABLE 4.—*Rawin observations by the Central Meteorological Observatory, Aug. 31–Sept. 1, 1949 (135th meridian civil time)*

Aug. 31, 0920			Aug. 31, 1220			Aug. 31, 1656			Aug. 31, 1840			Sept. 1, 1225		
Height m.	Direction degrees	Speed m/sec.	Height m.	Direction degrees	Speed m/sec.	Height m.	Direction degrees	Speed m/sec.	Height m.	Direction degrees	Speed m/sec.	Height m.	Direction degrees	Speed m/sec.
400	71	6.2	300	93	11.0	2000	166	9.0	370	110	7.9	350	196	8.0
800	97	13.0	600	87	14.0	2300	117	6.5	750	112	10.8	800	193	12.0
1050	109	12.5	900	90	18.0	2600	114	6.8	1100	124	11.0	1250	211	13.0
1350	119	9.5	1150	97	12.0	2900	173	7.8	1480	126	14.8	1700	217	14.0
1600	126	8.0	1400	115	11.0	3300	146	8.2	1830	136	13.4	2200	229	15.5
1850	126	5.5	1650	151	5.8	3700	149	6.5	2250	136	15.8	2700	232	12.5
2100	131	5.0	1900	180	7.5	4100	187	5.3	2550	141	13.5	3150	246	10.0
2350	118	7.2	2150	200	7.3	4550	187	8.2	2950	130	18.5	3600	259	8.5
2700	111	10.3	2400	239	8.6	4950	170	8.6	------	------	----	4100	264	6.5
3100	108	14.5	2650	262	5.0	5400	161	8.8	------	------	----	4600	275	6.0
3900	110	27.5	2900	260	4.5	5900	160	9.0	------	------	----	5050	284	6.0
4800	106	47.5	3150	216	5.0	6300	150	7.8	------	------	----	5500	269	6.5
5300	99	35.0	3400	180	2.8	6700	150	7.2	------	------	----	6000	287	7.5
5750	103	52.0	3650	157	5.4	7100	161	7.2	------	------	----	6450	304	7.0
6100	92	42.0	3900	143	6.9	7450	175	7.0	------	------	----	6900	336	5.8
6400	87	29.0	4150	142	8.3	7850	149	6.5	------	------	----	7400	315	4.5
6700	79	26.0	4400	142	9.3	8200	110	3.0	------	------	----	7900	275	4.5
7000	69	21.0	4700	136	13.0	8600	110	9.3	------	------	----	8350	237	10.5
7300	78	18.0	4950	135	11.5	9000	98	11.0	------	------	----	8800	218	8.0
7550	99	11.0	5200	135	15.0	9400	119	14.0	------	------	----	9300	200	7.0
7850	126	11.0	5400	126	17.0	9800	122	16.0	------	------	----	9800	184	9.0
8150	160	14.0	5650	135	13.2	10250	106	18.0	------	------	----	10200	160	10.2
8450	165	14.0	------	------	----	10700	95	11.5	------	------	----	10700	182	10.4
8750	165	19.0	------	------	----	11150	111	18.5	------	------	----	11200	200	10.0
9050	108	12.0	------	------	----	11650	106	22.2	------	------	----	11700	214	7.8
9400	100	17.0	------	------	----	12100	101	25.0	------	------	----	12100	181	5.5
9700	101	13.0	------	------	----	------	------	----	------	------	----	12600	271	9.5
10050	102	17.0	------	------	----	------	------	----	------	------	----	13100	238	6.8
10400	154	25.0	------	------	----	------	------	----	------	------	----	13600	254	6.5
10800	214	38.0	------	------	----	------	------	----	------	------	----	------	------	----
11150	222	37.0	------	------	----	------	------	----	------	------	----	------	------	----
11550	232	51.0	------	------	----	------	------	----	------	------	----	------	------	----
12000	270	69.0	------	------	----	------	------	----	------	------	----	------	------	----
12400	265	63.0	------	------	----	------	------	----	------	------	----	------	------	----
12900	262	41.0	------	------	----	------	------	----	------	------	----	------	------	----
13450	262	42.0	------	------	----	------	------	----	------	------	----	------	------	----

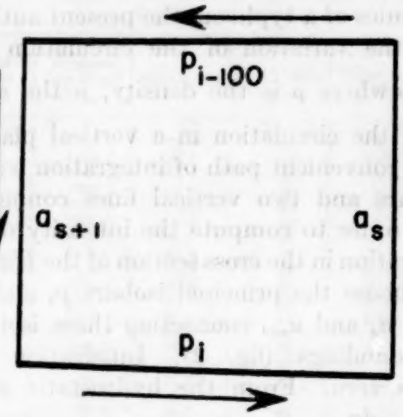

FIGURE 2.—Path of integration used in computing circulation acceleration. Circulation acceleration in the direction indicated by the arrows is taken to be positive.

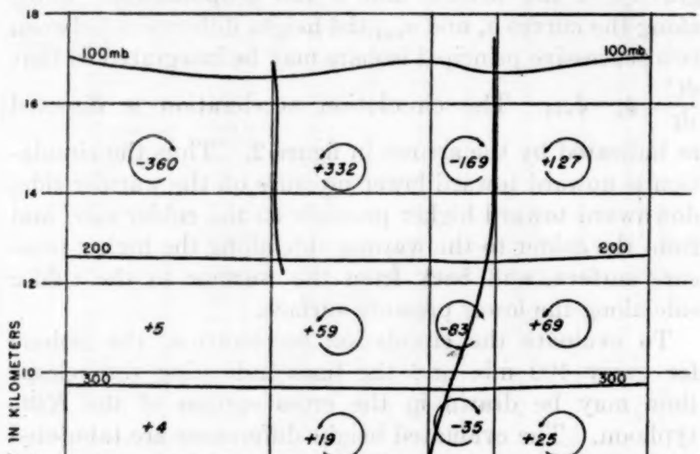

FIGURE 3.—Time cross section of the *Kitty* typhoon showing isobars (solid lines) and computed circulation accelerations. The number in each block formed by isobars and the thin vertical lines (times of release) is the circulation acceleration in meters. Blocks with circulation acceleration stronger than ±g·10m are designated by circular arcs, with arrow heads showing direction. The two heavy solid lines with considerable slope are the axes of low pressure.

each block in meters (geometrical height) instead of dynamic meters (geopotential). The descending motion in the core and the ascending motion in the storm region, must receive a retardation owing to the evaluated circulation acceleration, while the original baroclinicy loses its intensity. Thus the descending motion in the core and the ascending motion in the storm region are of *dynamic origin, other than the circulation acceleration.* The isobaric curves of figure 3 (and also table 5) show clearly that the amplitude of the pressure minimum is progressively decreased with increasing altitude in the troposphere. Above 12 to 13 km., such a tendency continues so that a maximum of pressure appears over the region of minimum pressure in the lower layers. The forward displacement of the pressure minimum at greater heights found by Simpson [6] seems to be real, and is largely a reversal from results of statistical investigations [7, 8] for extra-tropical cyclones. The heights of isobaric surfaces for each 100-mb. interval from the original soundings are printed in table 5.

TABLE 5.—*Heights for each principal isobaric surface in meters*

Date and hour (135th meridian civil time)	Aug. 31st					Sept. 1st	
	0904	1220	1330	1554	1849	0150	1100
1000 mb.	76	32	6	−4	*−74*	15	76
900	989	947	922	911	*838*	929	989
800	1993	1955	1927	1917	*1839*	1934	1995
700	3113	3075	3046	3037	*2956*	3061	3122
600	4381	4345	4318	4303	*4224*	4324	4390
500	5846	----	----	5763	*5691*	5776	5854
400	7589	----	----	7494	*7439*	7509	7594
300	9752	----	----	9632	*9612*	9663	9744
200	12628	----	----	*12439*	*12502*	*12494*	12570
100	17018	----	----	*16702*	*16934*	*16594*	17030

REFERENCES

1. Central Meteorological Observatory, Tokyo, *Aerological Data of Japan for August and September 1949.* (In preparation)
2. Central Meteorological Observatory, Tokyo, *Preliminary Reports on the KITTY Typhoon,* 1949. (In Japanese)
3. H. Yamada and S. Matsuhashi, *Vertical Structure of Typhoons,* 1950. (In Japanese)
4. Y. Masuda, "On the Method of Computing Vertical Motion in the Atmosphere (1st, 2nd, and 3rd reports)," *Papers in Meteorology and Geophysics,* vol. 1, No. 1, October 1950, pp. 1–28.
5. E. Palmén, "On the Formation and Structure of Tropical Hurricanes," *Geophysica,* No. 3, 1948, p. 26–38.
6. R. H. Simpson, "A Note on the Movement and Structure of the Florida Hurricane of October 1946," *Monthly Weather Review,* vol. 75, No. 4, April 1947, pp. 53–58.
7. C. M. Penner, "The Effects of Tropospheric and Stratospheric Advection on Pressure and Temperature Variations," *Canadian Journal of Research,* vol. A19, 1941, pp. 1–20.
8. B. Haurwitz, *Dynamic Meteorology,* McGraw-Hill, New York, 1941, pp. 322–325.

THE WEATHER AND CIRCULATION OF NOVEMBER 1950[1]

EUGENE J. AUBERT

Extended Forecast Section, U. S. Weather Bureau
Washington, D. C.

The Indian summer weather which prevailed over most of the country in October 1950 terminated abruptly early in November. The weather of November was spectacular in contrast to the more placid regime of the previous month. Both high and low daily temperature records were set in many localities; heavy rains caused widespread flooding and property damage in the Central Valley of California; and intense storminess caused snow depths to reach record proportions and paralyzed transportation facilities in the upper Ohio Valley.

The mean atmospheric circulation for the month in the vicinity of North America at the 700-mb. level (fig. 1) was characterized by a Gulf of Alaska Low with a trough and below normal heights extending southwestward to the Hawaiian Islands. A ridge was located over the western United States with 700-mb. heights higher than normal in the south but below normal in the north. A full latitude trough extending from northern Canada to Florida had its greatest intensity in the United States and was weaker than normal in Canada. A strong ridge with blocking characteristics was located east of Newfoundland in the western Atlantic.

[1] See Charts I–XI following p. 200, for analyzed climatological data for the month.

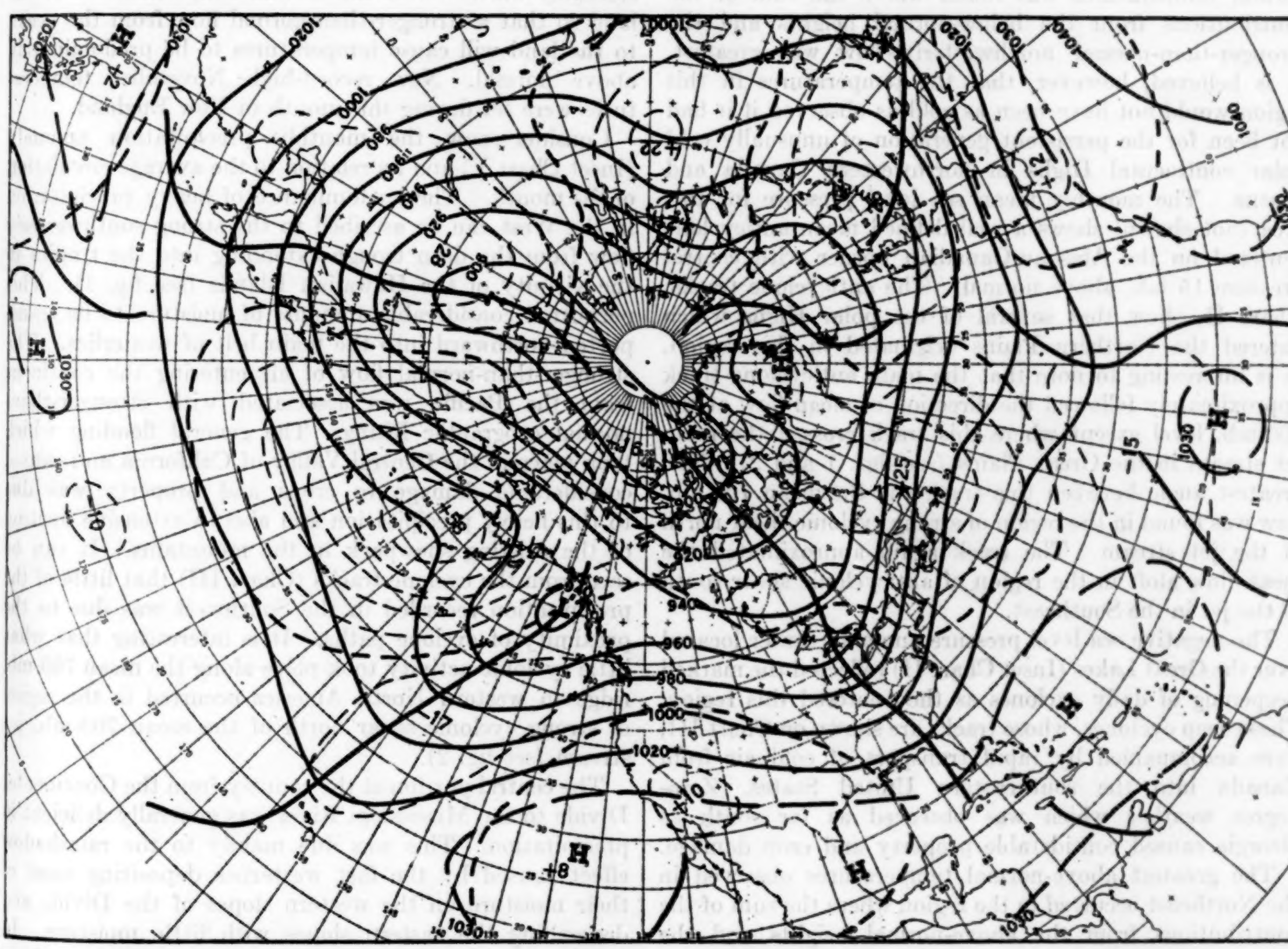

FIGURE 1.—Mean 700-mb. chart for the 30-day period October 31–November 29, 1950. Contours at 200-ft. intervals are shown by solid lines, 700-mb. height departures from normal at 100-ft. intervals by dashed lines with the zero isopleth heavier. Anomaly centers and contours are labeled in tens of feet. Minimum latitude trough locations are shown by heavy solid lines.

Other significant features of the mean atmospheric circulation are apparent from the average geostrophic wind field at the 700-mb. level (fig. 2). A well defined jet stream was located over the United States and the eastern Pacific. The wave pattern which was discussed with the aid of the 700-mb. height field is similarly apparent in the meanders of this jet. A secondary mean jet stream was located over northern Alaska and Canada.

The great contrast in the temperatures observed in different regions of the United States during the month can be seen from Chart I. Much above normal temperatures were recorded in the Northeast and Southwest while very cold weather occurred from the Northern Plains to Florida.

The warm weather in the Southwest was associated with the strong trough in the eastern Pacific. At the 700-mb. level (fig. 1), the mean trajectory of air came from the tropics. The above-normal 700-mb. heights were also associated with the warm temperatures.

The low temperatures observed from the Northern Plains to Florida may also be interpreted with the aid of the 700-mb. circulation. The belt of maximum below-normal temperatures was found where the sum of the contributions from the below-normal heights and the stronger-than-normal northwesterly flow was greatest. It is believed, however, that the temperatures in this region would not have been as cold as observed if it had not been for the persistent generation of unusually cold polar continental Highs in northwestern Canada and Alaska. The monthly mean sea level pressure for this area (not shown) shows a well defined mean anticyclone centered on the Alaskan-Canadian border with central pressure 15 mb. above normal. The anticyclone tracks, Chart II, show that several of the polar Highs which entered the Northern Plains originated in this region. It is interesting to note that the main anticyclone track approximately followed the direction of mean flow at the 700-mb. level except where this track crossed the main jet stream in the Great Plains (see figs. 1 and 2). The greatest angle between this track and the mean 700-mb. flow was found in the region of strong cyclonic shear north of the jet stream. The track again approximated the mean flow aloft in the region of anticyclonic shear south of the jet in the Southeast.

The negative sea level pressure anomaly center located over the Great Lakes (Inset Chart II) reflected the marked deepening of daily cyclones as they entered this region. These deep cyclones, whose tracks are shown on Chart III, were accompanied by rapid transport of cold air from Canada into the southeastern United States. Zero-degree weather which was observed as far south as Georgia caused considerable property and crop damage.

The greatest above-normal temperatures observed in the Northeast occurred in the region where the sum of the contributions from the above-normal heights and the strong relative-to-normal southeasterly flow at the 700-mb. level was greatest. At sea level, a stronger-than-normal southeasterly flow was observed. In November, the ocean temperatures along the east coast are considerably warmer than the normal temperatures over the land so that a stronger-than-normal flow from the ocean to the land will cause temperatures to be predominately above normal. New record-high November temperatures were set during this month in New England.

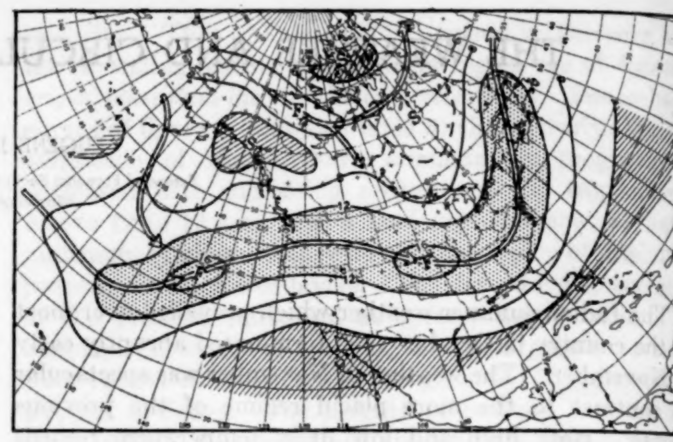

FIGURE 2.—Mean geostrophic (total horizontal) wind speed at 700 mb. for the 30-day period October 31–November 29, 1950. Isotachs at 4-m. p. s. intervals are shown by solid lines while the axes of maximum wind speeds (jets) are shown by double lines.

Consider now the monthly precipitation anomaly (Inset Chart V) and its relation to the average circulation of the month. The predominance of heavy precipitation in the West can be ascribed to the strong southwesterly flow from the deep trough extending into the tropics in the vicinity of the Hawaiian Islands (see fig. 1). This permitted considerable amounts of moisture to be transported northward into the main belt of westerlies. The stronger-than-normal flow of air entering the continent from the Pacific was associated with stronger-than-normal orographic lifting. The general flooding which took place in the Central Valley of California and caused considerable damage to crops and property was due to this heavy precipitation and also to extensive melting of the existing snowpack in the mountains. It can be seen from the cyclone tracks (Chart III) that little of the precipitation recorded in the Southwest was due to the proximity of cyclone paths. It is interesting that what little cyclonic activity took place along the mean 700-mb. ridge in western North America occurred in the region of strong cyclonic shear north of the mean 700-mb. jet stream (see fig. 2).

The central portion of the country from the Continental Divide to the Mississippi River was generally deficient in precipitation. This was due mainly to the rainshadow effect caused by the fast westerlies depositing most of their moisture on the western slopes of the Divide and descending the eastern slopes with little moisture. In the southern part of this region there was little cyclonic

activity and a pronounced anticyclonic shear aloft. This was associated with drought conditions in Texas and New Mexico where many stations recorded little or no precipitation for the entire month and supplemental feeding was required for cattle. In the Northern Plains generally normal amounts of precipitation were recorded mainly in the form of snow (see Chart VII). Here the effect of the downslope flow was counteracted by the proximity of the storm track, the strong cyclonic shear aloft, and the easterly wind components at sea level relative to normal (Chart III inset).

Precipitation was deficient in the Southeast. It appears that little moist tropical air entered this region, because of the northerly flow relative to normal at the 700-mb. level (see fig. 1) and the slight reverse tilt to the trough (NNW-SSE).

The Ohio Valley and the Northeast generally received excessive amounts of precipitation much of which was in the form of snow (see Chart VII). Snow depths in western Pennsylvania, eastern Ohio, and West Virginia reached record proportions (1 to 3 feet) blocking highways and paralyzing city transportation. A deep 700-mb. mean trough with considerable trough-ridge amplitude was located in the western portion of this area and a negative pressure anomaly center was observed both at sea level (Inset Chart II) and aloft (fig. 1). Considerable mean cyclonic vorticity is apparent in the flow in this region, as can be seen from the curvature of the sea level isobars (Chart VI), and 700-mb. contours (fig. 1) as well as the horizontal wind shear shown in figure 2.

The direction of cyclone tracks for the month over eastern North America (Chart III) might at first glance appear chaotic. Once one realizes that the ridge east of Newfoundland had strong blocking characteristics at the end of the month, however, a regular transition in the direction of the cyclone paths becomes apparent. At the beginning of the month, cyclones traversed eastern North America moving toward the east and northeast. The latter half of the month, when blocking was active, cyclones traveled toward the north and even northwest, causing new snowfall records in the upper Ohio Valley and winds of hurricane velocity (gusts to over 100 m. p. h.) in the Northeast. (See article by Smith on the following pages.)

THE DESTRUCTIVE STORM OF NOVEMBER 25–27, 1950

CLARENCE D. SMITH, JR.
WBAN Analysis Center, U. S. Weather Bureau
Washington, D. C.

The weather over central and eastern United States during November 1950 was notable in several respects. The most outstanding was the rapid intensification of a small Low into one of the most destructive storms ever recorded in northeast United States. This report describes the life history, contributions to deepening, and effects of this storm.

LIFE HISTORY OF THE STORM

The storm of November 25–27 was first noted on the surface weather map of 1230 GMT, November 24 as a small Low developing over North Carolina and western Virginia (fig. 1). The cold front on which the Low formed had moved rapidly southward and eastward from a position on November 22 through Montana and North Dakota. The old occluded Low in the Great Lakes region, which had been one of the major factors in the weather situation, was filling rapidly. By 0030 GMT, November 25 (fig. 2), it was obvious that the deepening Low over North Carolina had completely captured a place of prominence over the Low in the Lakes region.

Some factors contributing to that change can be seen in the 500-mb. charts. Figure 3, the 500-mb. chart for 0300 GMT, November 24, shows the well-developed upper level Low associated with the filling surface storm over the Lakes region. Prior to that time the 500-mb. contours and isotherms had been nearly concentric indicating a cold-core Low with but little temperature advection. The past positions in figure 3 show that the movement of the Low had been quite regular. By 0300 GMT, November 24 (fig. 3), however, the isotherms showed the coldest air over Iowa southwest of the center. The 500-mb. chart for 0300 GMT, November 25 (fig. 4) shows that the cold air was swept rapidly around the Low and was associated with a sudden southward elongation of the center. During the period 0300 GMT, November 24 to 0300 GMT, November 25, the 500-mb. height at Nashville, Tenn., fell 1,140 feet and at Atlanta, Ga., 1,110 feet, while the temperature fell 10° C. and 9.3° C. respectively. Rapid warming aloft also occurred over Minnesota to the northwest of the Low. The 500-mb. temperature at St. Cloud, Minn., for example, rose from −37.6° C. at 0300

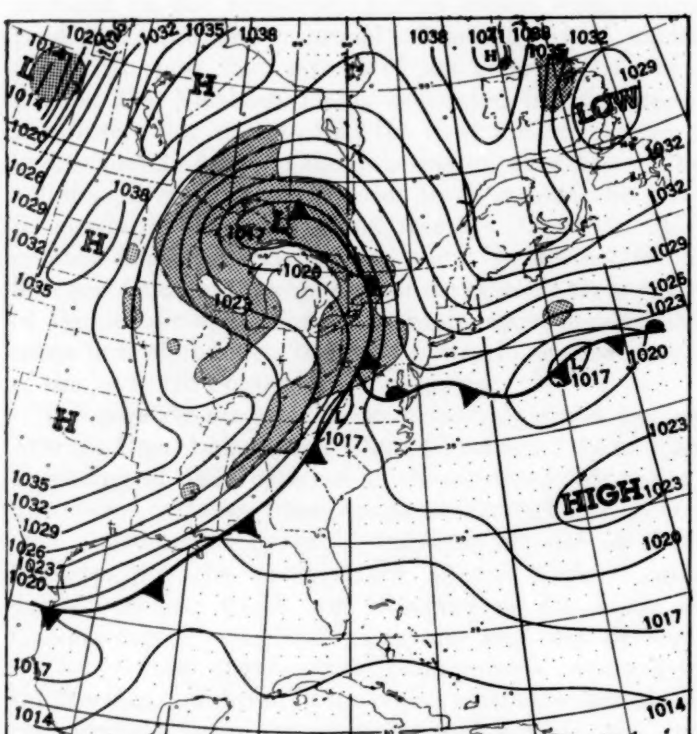

FIGURE 1.—Surface weather chart for 1230 GMT, November 24, 1950. Shading indicates areas of active precipitation.

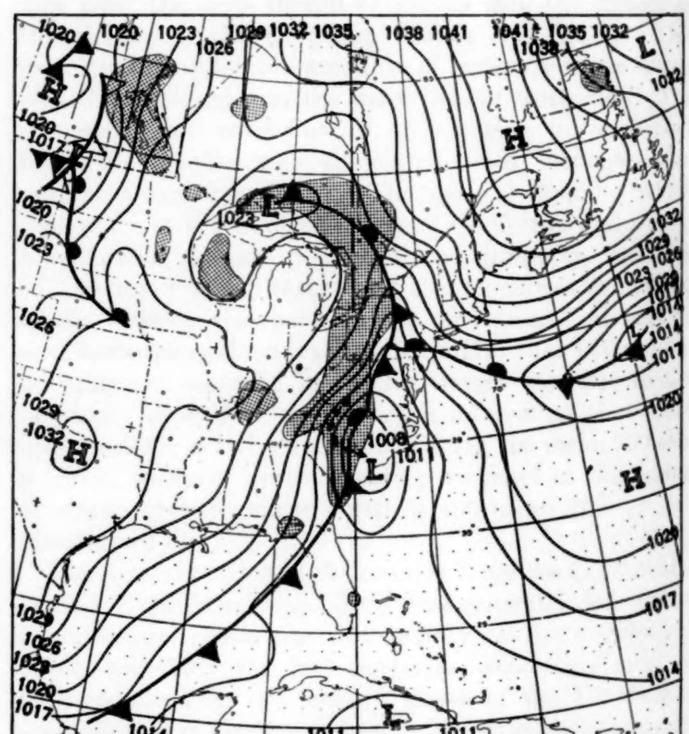

FIGURE 2.—Surface weather chart for 0030 GMT, November 25, 1950. Small squares connected by arrows indicate past positions of main Low at 12-hour intervals.

GMT, November 24 to −19.5° C. at 0300 GMT November 25. Strong warm advection similiar to this is often associated with rapidly moving Lows because they tend to have an intensifying warm ridge following them.

A close examination of the 500-mb. wind field at 1500 GMT, November 24 (not shown) revealed north winds of 80–85 knots on the west side of the Low. The contour gradient downstream on the south side of the Low was not sufficiently strong to cause air at those speeds to follow the curve of the contours. Consequently the air passing into the southern side of the Low crossed contours toward greater contour heights, contributing to the production of northerly winds over Illinois, western Kentucky, and western Tennessee, and consequently to the elongation of the Low [1].

By these means the Low was enabled to re-form quickly over North Carolina by 1500 GMT, November 25 (not illustrated, see figure 7 for 0300 GMT of the 26th), further reinforcing the surface Low in that vicinity in preference to the old Low in the Lakes region.

By 1230 GMT, November 25 (fig. 5) the surface Low had deepened 26 mb. Surface winds behind the former occlusion through Pennsylvania and New York were changed to northerly with some easterly component, the occlusion becoming a warm front. Close examination of a large scale surface map for 1530 GMT, November 25 (not reproduced) revealed signs of a new Low forming near Erie, Pa. By 0030 GMT, November 26 (fig. 6), the new center was the main center and was located near Cleveland, Ohio. The central pressure was 983 mb., 8.4 mb. lower than the original center 12 hours earlier.

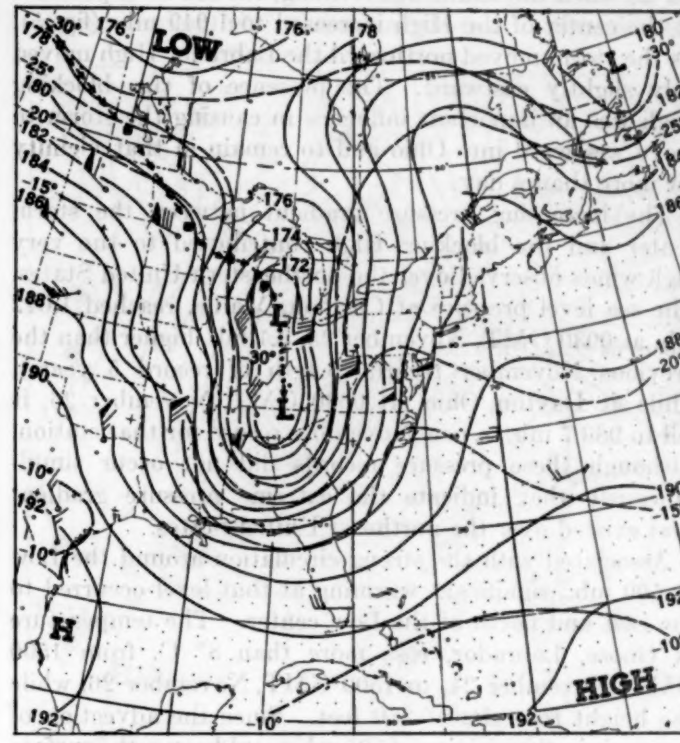

FIGURE 4.—500-mb. chart for 0300 GMT, November 25, 1950. Dotted portion of the Low track represents reforming of low center.

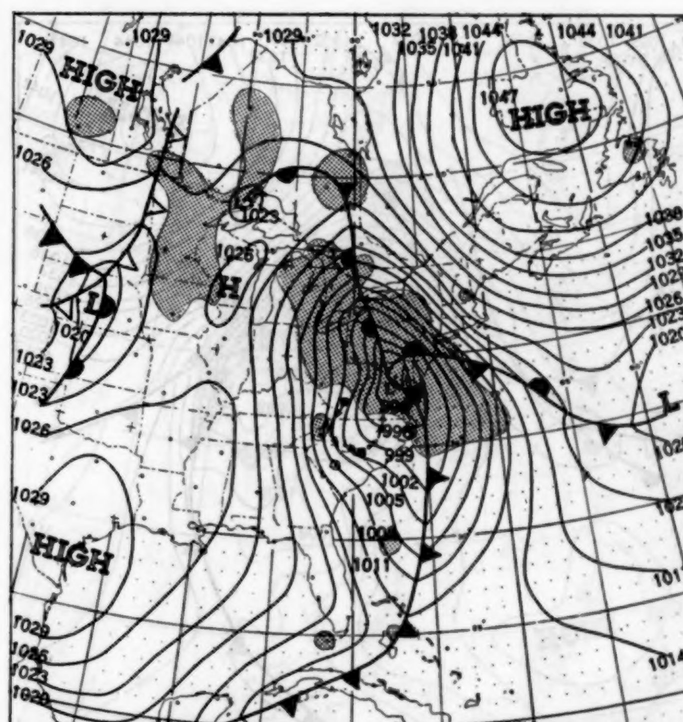

FIGURE 5.—Surface weather chart for 1230 GMT, November 25, 1950.

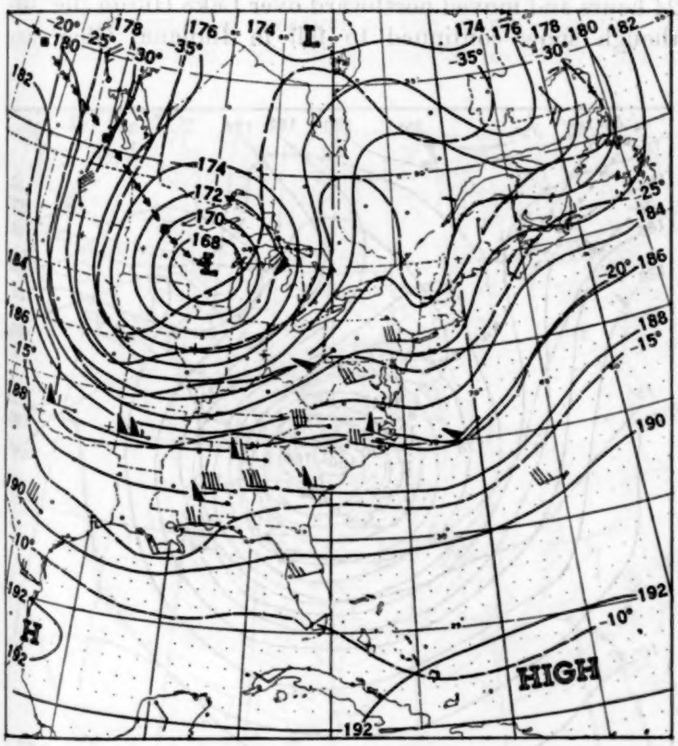

FIGURE 3.—500-mb. chart for 0300 GMT, November 24, 1950. Contours (solid lines) at 200-foot intervals are labeled in hundreds of geopotential feet. Isotherms (dashed lines) are at intervals of 5° C. Barbs on wind shafts are for speeds in knots (pennant=50 knots, full barb=10 knots and half barb=5 knots). Past positions of the main Low are at 12-hour intervals.

Some explanation of the redevelopment of the center to the west is seen by studying the High which existed at low levels over the Labrador region. During the period 1230 GMT, November 24 to 1230 GMT, November 25 when the storm was forming, the sea level pressure at the center of the High increased to 1,049 mb. (fig. 5). As the storm moved northward the Labrador High moved only slightly eastward. The presence of this blocking High was an important influence in causing the storm to move westward into Ohio and to remain in that vicinity for more than a day.

The increasing pressure gradient between the storm center and the blocking High contributed to the very high winds observed over the northeastern United States. The sea level pressure at Caribou, Maine, reached 1,042 mb. at 0930 GMT, November 25, 3.1 mb. higher than the previous November record (length of record 5 years), while at Dayton, Ohio, at 0630 GMT, November 26, it fell to 983.7 mb., a new November record for that station. Although these pressure records did not occur simultaneously they indicate the extreme pressure gradient that existed over the northeast United States.

Associated with the strong circulation around the Low at 500 mb., significant warming at that level occurred to the east and north of the Low center. The temperature at Goose, Labrador, rose more than 8° C. from 1500 GMT, November 24, to 1500 GMT, November 26, while the height rose almost 850 feet. Since the advection of warm air in the vicinity of 500 mb. would cause the surface pressure to fall (other factors being unchanged) it is necessary to look elsewhere for a cause of the rising surface pressures and 500-mb. heights. A study of the 200-mb. charts shows that associated with the southerly circulation over the east coast, the temperature at that level over Goose, Labrador, fell almost 15° C. from 1500 GMT, November 24, to 1500 GMT, November 26, while the height rose more than 1,000 feet. Apparently the movement of relatively colder and heavier air in the stratosphere over the Labrador region compensated for the relatively warmer and lighter air brought in around 500 mb. and allowed the surface pressure to remain about the same. Thus the circulation of the Low itself influenced its future movement by contributing to the maintenance of the blocking High.

While the surface Low re-formed and deepened over Ohio, the 500-mb. Low reached its lowest central value, approximately 16,550 feet, at 0300 GMT, November 26 (fig. 7). The past positions, at 12-hour intervals as shown in figure 7, indicate the 500-mb. Low was circling northward. By 0300 GMT, November 27 (fig. 8), it was centered northeast of Toledo, Ohio. Subsequently it moved slowly northward, re-formed over Lake Erie on November 28, moved southward over Washington, D. C., and off toward the northeast. The surface Low reached its maximum depth at 0630 GMT, November 26, over northern Ohio with a central pressure of 978 mb., and by 1230 GMT, November 26, was centered just northeast of Columbus, Ohio (fig. 9). It filled rapidly in the following 24 hours and moved northward over Lake Huron (fig. 10), though snow continued to fall in Indiana, Ohio, and

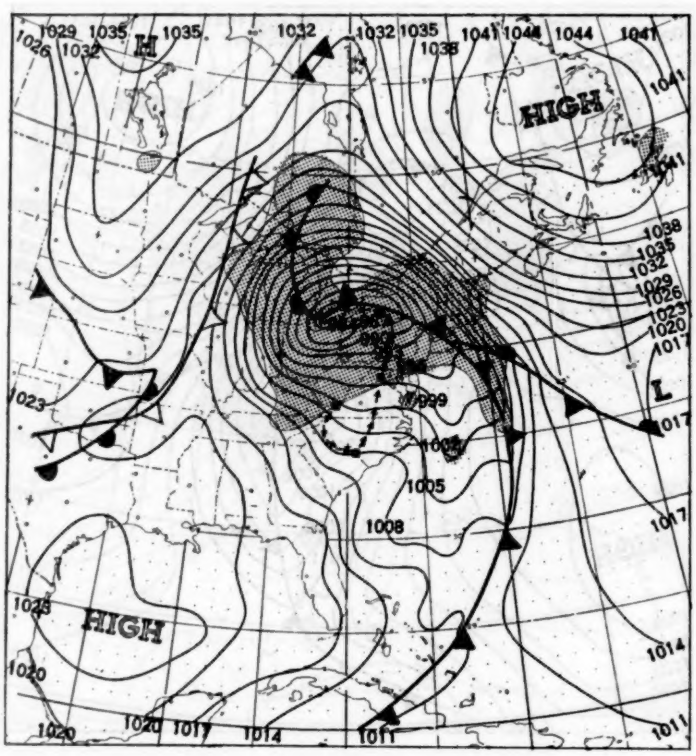

FIGURE 6.—Surface weather chart for 0030 GMT, November 26, 1950.

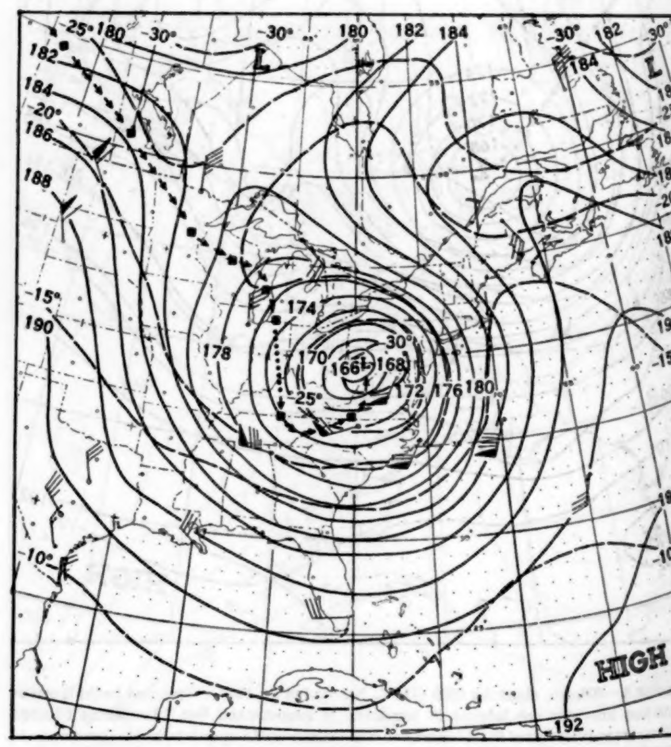

FIGURE 7.—500-mb. chart for 0300 GMT, November 26, 1950.

Pennsylvania. Before completely filling, the Low circled southward again through Ohio, further prolonging the snow showers.

CONTRIBUTIONS TO DEEPENING OF THE STORM

Vederman [2] studied changes in the thickness of the standard layers over the moving centers of rapidly deepening Lows in the eastern United States. His results showed "that the lower two-thirds by weight of the central column becomes thinner (colder and denser) as a storm deepens. The upper one-third of the central column becomes 'thicker' and warmer by an amount sufficient to counteract the action of the lower layers and an additional amount to deepen the Low". A similar analysis of this storm shows that for the 24-hour period ending 1500 GMT, November 25, when the surface Low deepened 24 mb., the entire central column up to 100 mb. became thicker and warmer. This would leave only the portion of the atmosphere above 100 mb. to act in the opposite sense. For the 24-hour period ending 0300 GMT, November 26, when the Low deepened 22 mb., the standard layers below 300 mb. became thinner and colder while the layers above 300 mb. became thicker and warmer. The results for the latter period are entirely compatible with Vederman's average results while those for the former period are perhaps more representative of what might be called an "ideal" case of deepening.

The geographical location of the storm and the distribution of warm and cold air masses probably offer an explanation for the warming in the former period. The Low formed over the Atlantic Coast States not far from the large source of relatively warm, maritime air over the ocean. Also, the existence of a blocking High over Labrador caused the sea level pressure gradient and the contour gradient aloft to become steepest in the northeast

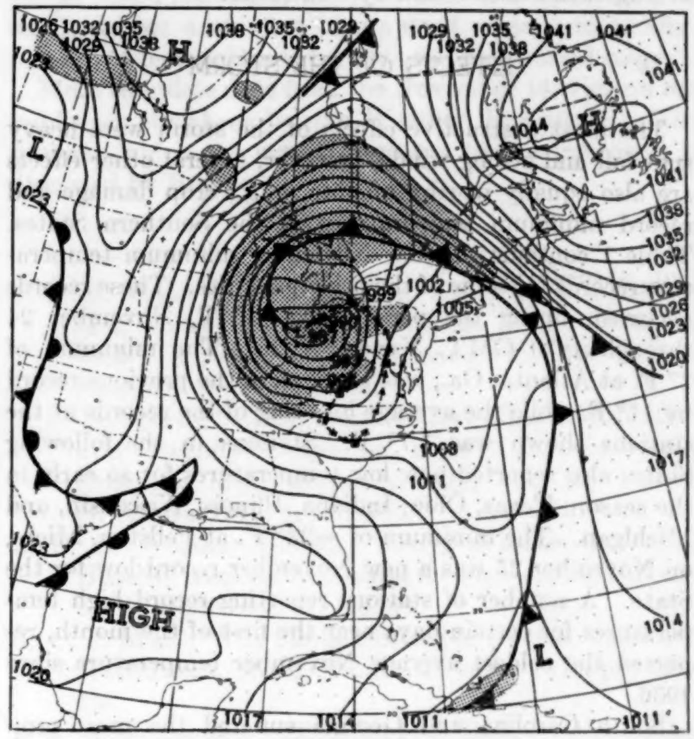

FIGURE 9.—Surface weather chart for 1230 GMT, November 26, 1950.

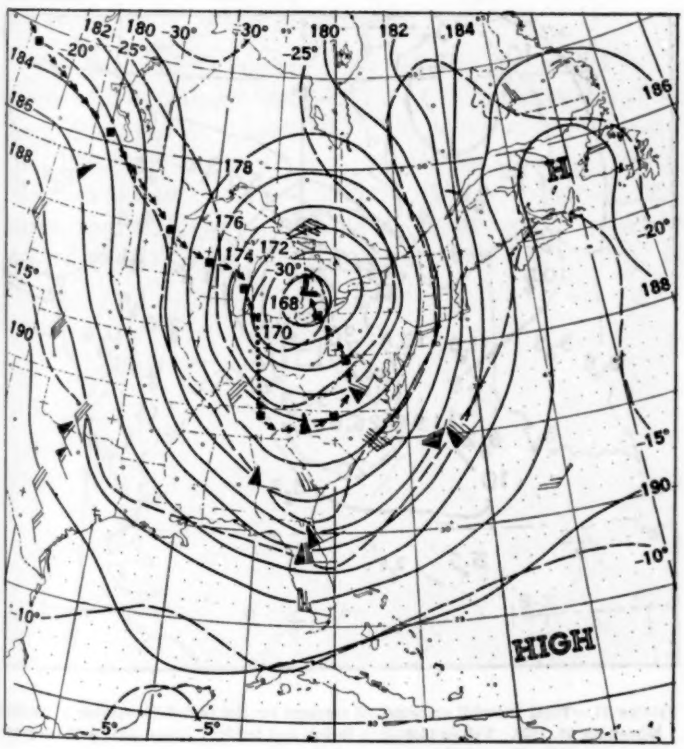

FIGURE 8.—500-mb. chart for 0300 GMT, November 27, 1950.

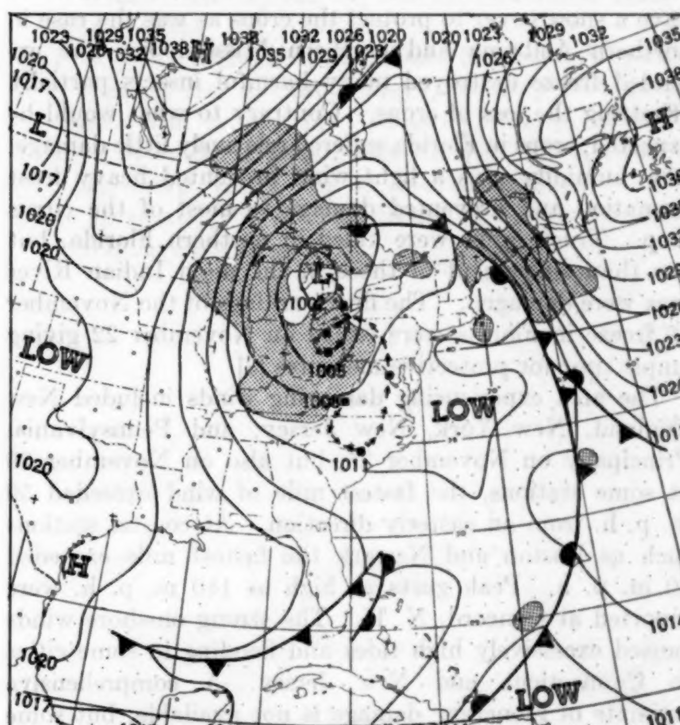

FIGURE 10.—Surface weather chart for 1230 GMT, November 27, 1950.

quadrant producing rapid influx of the warm air. The advection of colder air in the low levels was generally with winds less strong than those in the warm air and was delayed by the Appalachian Mountain barrier to some extent. It appears that after 12 hours of deepening the vertical mass distribution adjusted to agree with the average conditions found by Vederman.

EFFECTS OF THE STORM

The most destructive effects of the storm were heavy snowfall and strong winds, however, several other effects are also equally worthy of note, e. g., crop damage and record minimum temperatures in the Southern States. Table 1 contains the new November minimum temperature records for some of the principal cities. These records occurred during the period 1830 GMT, November 24 through 1830 GMT, November 25. The minimum of 3° F. at Atlanta, Ga., was lower than the previous record by 11° F. while the average lowering of the records at the stations shown was 5.7° F. Stations in the following States also reported new low temperatures for so early in the season: Texas, Ohio, Indiana, Illinois, Wisconsin, and Michigan. The minimum of −23° F. at Pellston, Mich., on November 25 was a new November record low for the State. A number of stations reporting record high temperatures for certain days near the first of the month, reported the coldest average November temperature since 1936.

South Carolina and Georgia suffered the most crop damage. Each had a period of several days that was colder than any November period on record but did not have a snow cover to protect the crops as was the case in northern Alabama and northern Mississippi. The extended freeze destroyed many harmful insects partially offsetting the loss of crops. Contrary to what would be expected, crops in Florida suffered relatively little damage. Low humidity plus a light wind prevented heavy frost formation and prevented damage to most of the citrus crop. Truck crops were killed in northern Florida, but less than 10 percent of those in the main Indian River area were damaged. The first warnings of the November 26 freeze in Florida were issued on November 22 giving ample time for protective measures [3].

The area experiencing damaging winds included New England, New York, New Jersey, and Pennsylvania. Principally on November 25, but also on November 26 at some stations, the fastest mile of wind exceeded 50 m. p. h. from an easterly direction. At coastal stations such as Boston and Newark the fastest mile exceeded 80 m. p. h. Peak gusts as high as 110 m. p. h. were reported at Concord, N. H. The strong on-shore winds caused excessively high tides and flooding in some cities in Connecticut and New Jersey. A comprehensive estimate of monetary damage is not available, but some areas reported more damage than resulted from the 1938 or 1944 hurricanes. According to news reports by insurance companies, payments to policy holders for storm damage aggregated more than for any previous storm in the United States.

The area receiving the largest amount of snow was centered in West Virginia, western Pennsylvania, and

TABLE 1.—*Some November minimum temperature records*

Station	Nov. 1950 minimum	Previous Nov. record minimum	Years of record
	° F.	° F.	
ALABAMA			
Birmingham	5	14	54
Mobile	22	24	78
Montgomery	13	18	70
FLORIDA			
Apalachicola	24	28	29
Jacksonville	23	25	79
Pensacola	22	25	70
GEORGIA			
Atlanta	3	14	72
Augusta	11	21	78
Savannah	15	22	79
KENTUCKY			
Louisville	−1	1	78
NORTH CAROLINA			
Asheville	−5	4	47
Wilmington	16	20	80
SOUTH CAROLINA			
Charleston	17	23	79
Greenville	11	14	65
TENNESSEE			
Chattanooga	4	11	72
Knoxville	5	8	79
Memphis	9	16	78
Nashville	−1	8	78

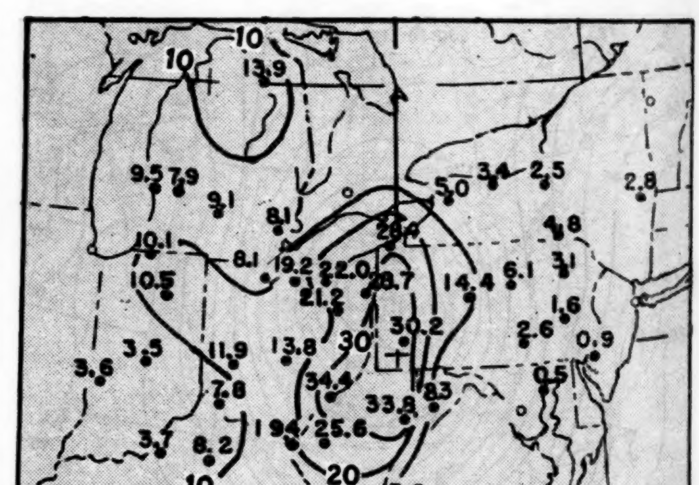

FIGURE 11.—Total snowfall at principal stations for the period November 24 through November 28, 1950. Values plotted in inches and tenths. Lines outline the approximate areas of 10-, 20-, and 30-inch accumulation.

eastern Ohio. Figure 11 shows the total amount that fell at certain principal stations during the period November 24–28. Table 2 contains some comparisons with previous snowfall records. The 34.4 inches that fell at Parkersburg, W. Va., during the 5-day period exceeded not only the record November amount but also the record monthly amount by 5.3 inches. The heavy snowfall plus drifting blocked the highways, railroads, and city streets in Ohio, West Virginia, western Pennsylvania, and parts of Indiana. Business and transportation were brought to a standstill. Many of the heavy industries in the Cleveland and Pittsburgh areas were forced to close. According to press reports the storm caused approximately 300 deaths either directly or indirectly. The electric power transmission lines were very severely damaged in the area of heavy snow resulting in more than 1,000,000 homes being without power for many days.

TABLE 2.—*Some snowfall comparisons*

Station	Snowfall November 24–28	Previous record November snowfall	Record monthly snowfall (all months)	Years of record
OHIO	*in.*	*in.*	*in.*	
Cincinnati	7.8	8.9	21.4	65
Cleveland	22.0	22.2	30.5	63
Columbus	13.8	8.2	29.2	65
Sandusky	19.2	8.6	29.8	66
Toledo	8.1	12.0	26.2	65
Youngstown	28.7	12.2	30.1	6
PENNSYLVANIA				
Curwensville	14.4	9.9	41.1	7
Erie	28.4	35.1	53.6	65
Pittsburgh	30.2	14.7	36.3	65
WEST VIRGINIA				
Elkins	33.8	20.5	36.6	51
Huntington	19.4	.4	19.1	9
Parkersburg	34.4	15.9	29.1	62
Petersburg	8.3	3.0	15.6	5

The storm of November 1950 has been compared to the storm of November 9 and 10, 1913. (The latter storm has been discussed by Mook [4].) The 1913 storm exceeded the 1950 storm in damage to Great Lakes shipping. Whereas the 1950 storm caused negligible damage to Lakes ships, the 1913 storm took 200 lives on Lake Huron and caused nearly $2,000,000 damage to Lakes ships [5]. In most sections the amount of snow in the 1950 storm exceeded the amounts in the 1913 storm [6].

The heavy snow of the 1950 storm, remaining on the ground approximately a week, was melted during the first 4 days of December by above-normal temperatures. Moderate flooding resulted in the Ohio River and tributaries. At Pittsburgh, the river stage reached 28.5 feet on December 4, 4½ feet above flood stage, and at Cincinnati, 56 feet on December 11, 4 feet above flood stage.

More complete data from the November 1950 storm are published elsewhere by the Weather Bureau [7]. The problem which the storm presented to the forecaster is discussed by Bristor [8].

REFERENCES

1. H. B. Wobus and L. C. Norton, "Some Synoptic Aspects of a Change in Weather Regime during February 1950", *Monthly Weather Review*, vol. 78, No. 2, February 1950, p. 31–40.
2. J. Vederman, "Changes in Vertical Mass Distribution over Rapidly Deepening Lows", *Bulletin of the American Meteorological Society*, vol. 30, No. 9, November 1949, p. 303–309.
3. U. S. Weather Bureau, *Weekly Weather and Crop Bulletin, National Summary*, for week ending November 28, 1950, vol. 37, No. 48.
4. C. P. Mook, "The Famous Storm of November, 1913", *Weatherwise*, vol. 2, No. 6, December 1949, pp. 126–128.
5. J. H. Armington, "Climatological Data for November, 1913, District No. 4, The Lake Region", *Monthly Weather Review*, vol. 41, No. 11, November 1913, p. 1678–1680.
6. F. J. Walz, "Climatological Data for November, 1913, District No. 3, Ohio Valley", *Monthly Weather Review*, vol. 41, No. 11, November 1913, p. 1666.
7. U. S. Weather Bureau, *Climatological Data, National Summary*, vol. 1, No. 11, November 1950.
8. C. L. Bristor, "The Great Storm of November 1950", *Weatherwise* (in press).

U. S. GOVERNMENT PRINTING OFFICE: 1951

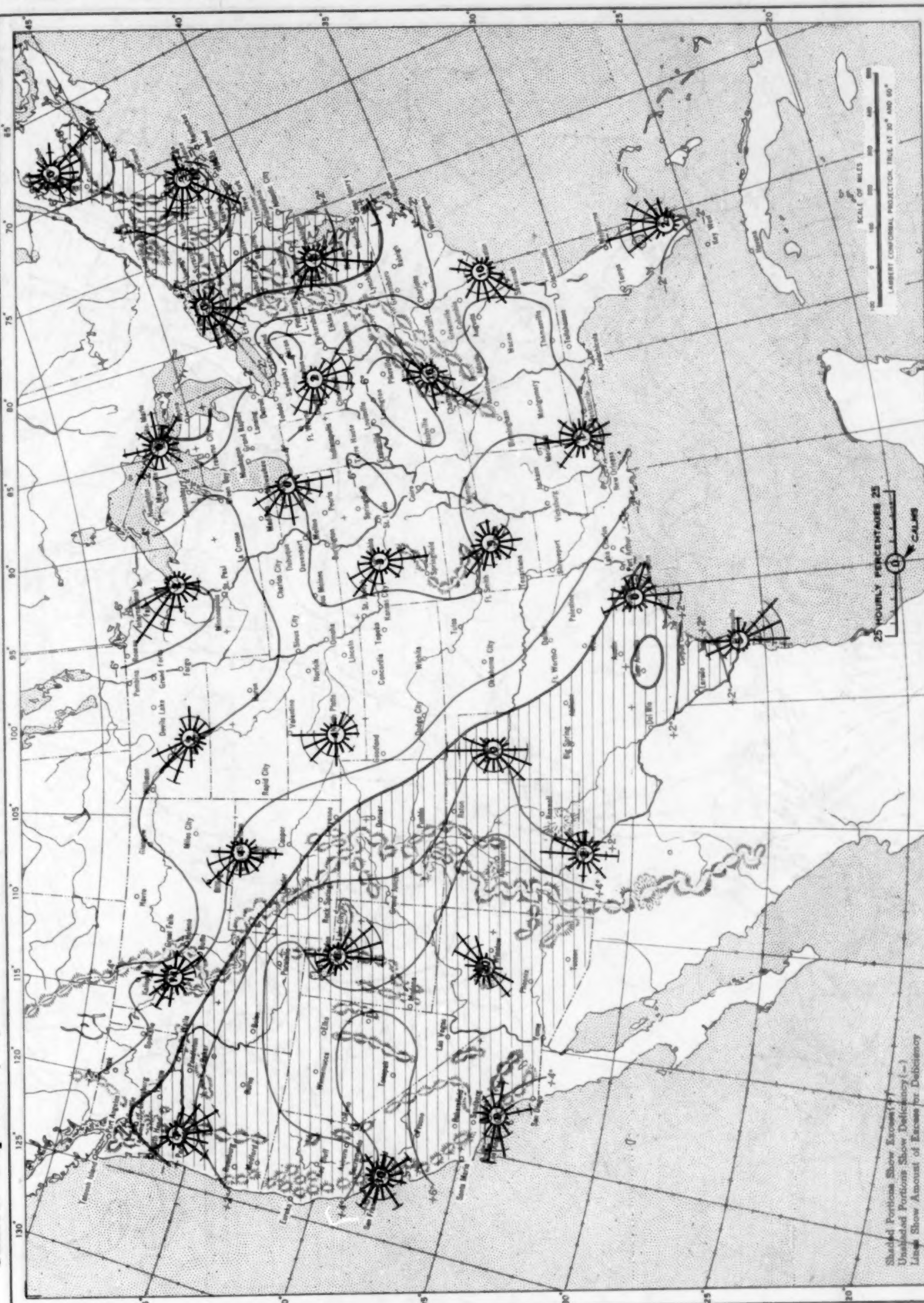

Chart I. Departure (°F.) of the Mean Temperature from the Normal, and Wind Roses for Selected Stations, November 1950

Chart II. Tracks of Centers of Anticyclones, November 1950. (Inset) Departure of Monthly Mean Pressure from Normal

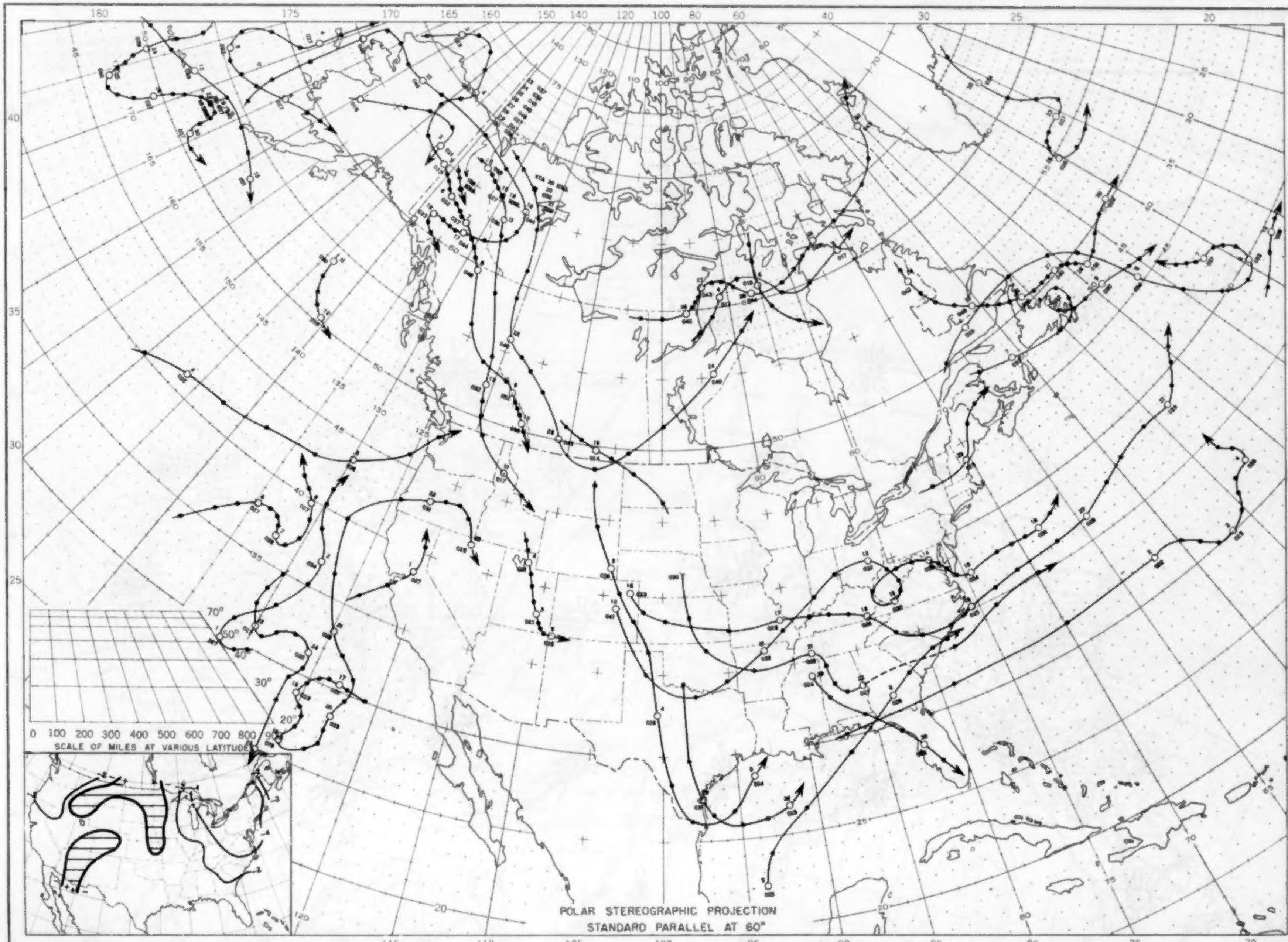

Circle indicates position of anticyclone at 7:30 a. m. (75th meridian time). Figure above circle indicates date, and figure below, pressure to nearest millibar. Dots indicate intervening 6-hourly positions. Square indicates position of stationary center for period shown. Only those centers which could be identified for 24 hours or more are included.

Chart III. Tracks of Centers of Cyclones, November 1950. (Inset) Change in Mean Pressure from Preceding Month

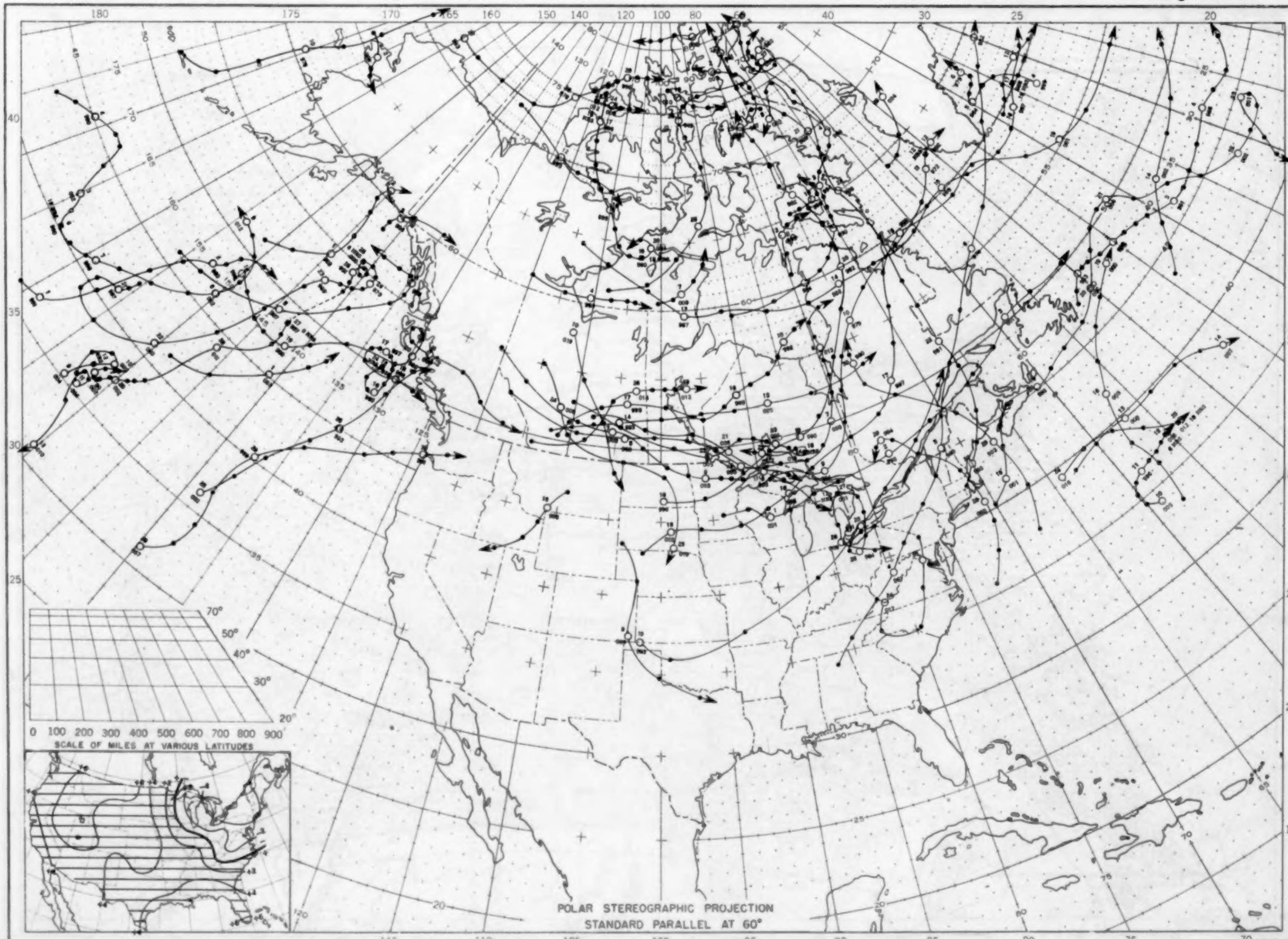

Circle indicates position of cyclone at 7:30 a. m. (75th meridian time). Figure above circle indicates date, and figure below, pressure to nearest millibar. Dots indicate intervening 6-hourly positions. Square indicates position of stationary center for period shown. Only those centers which could be identified for 24 hours or more are included.

Chart IV. Percentage of Clear Sky Between Sunrise and Sunset, November 1950

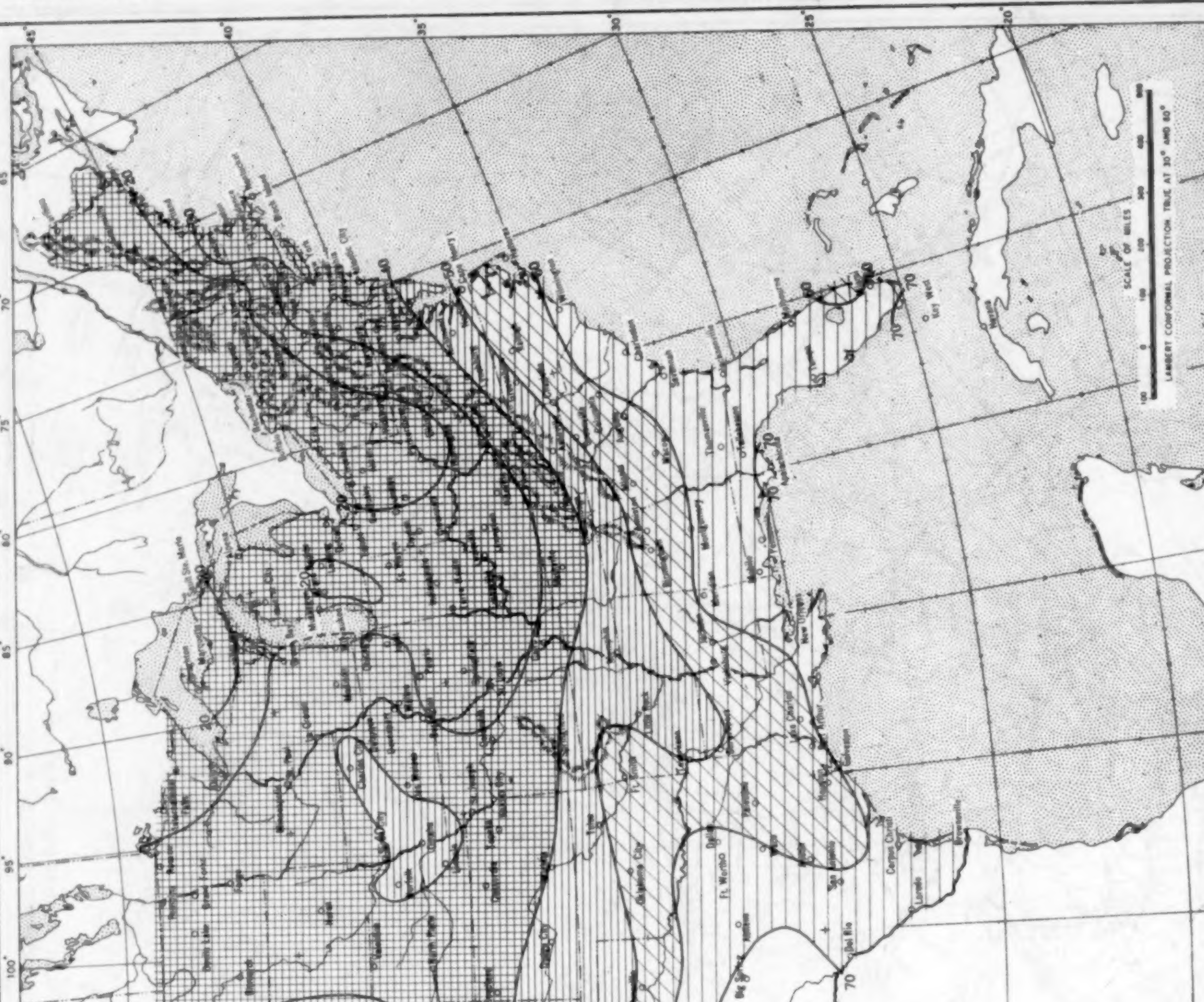

Chart V. Total Precipitation, Inches, November 1950. (Inset) Departure of Precipitation from Normal

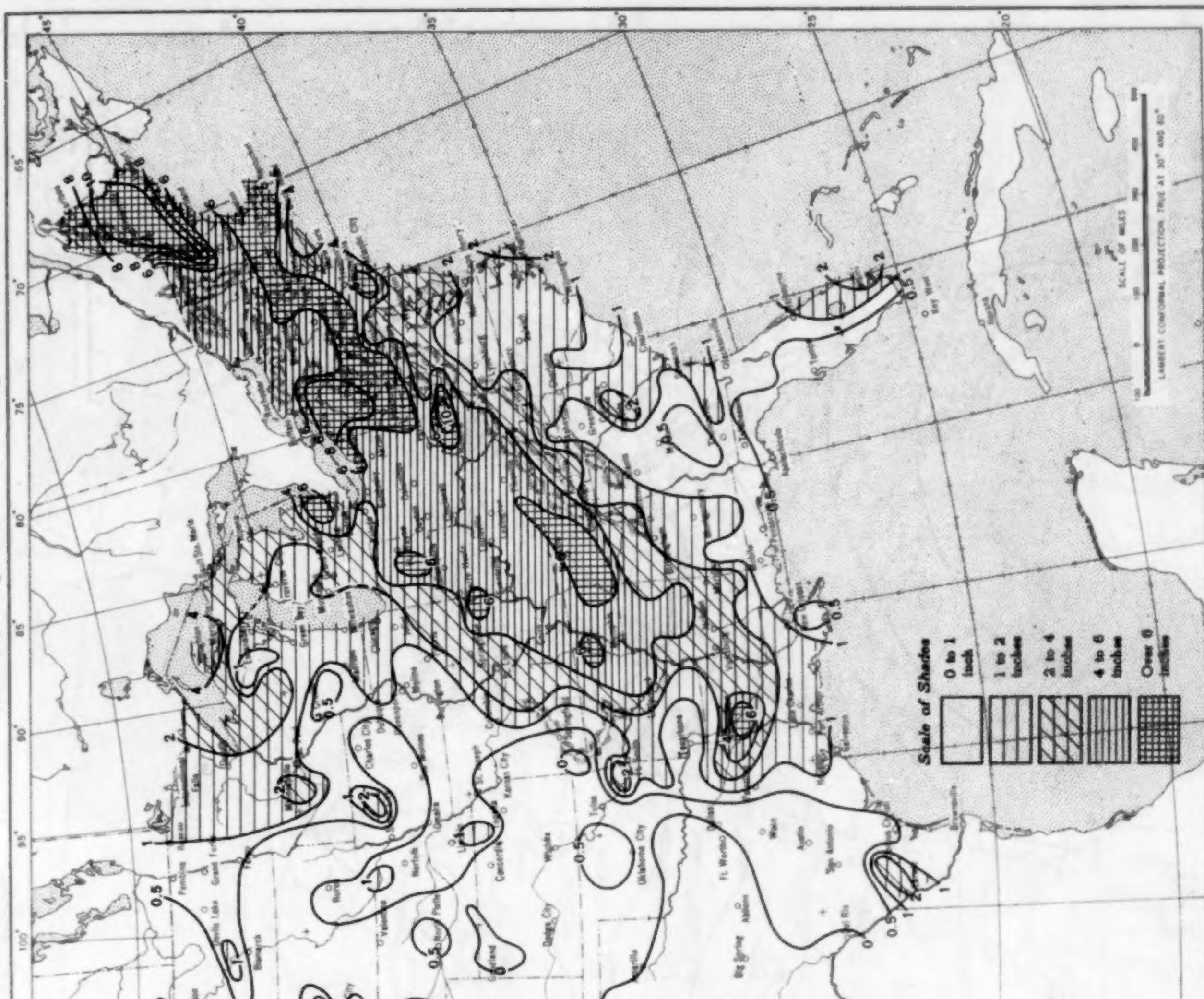

Chart VI. Mean Isobars (mb.) at Sea Level and Mean Isotherms (°F.) at Surface., November 1950

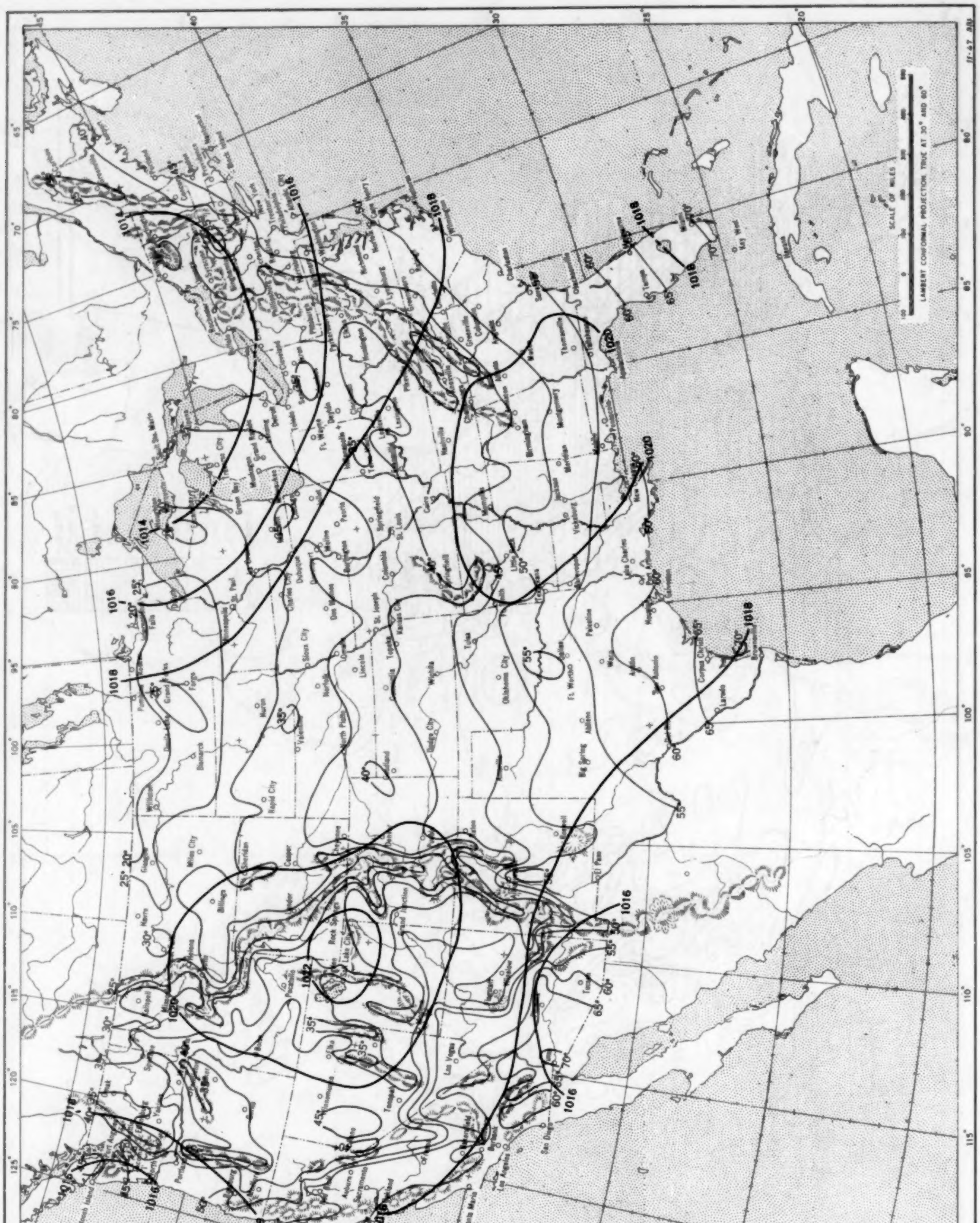

Chart VII. Total Snowfall, Inches, November 1950.

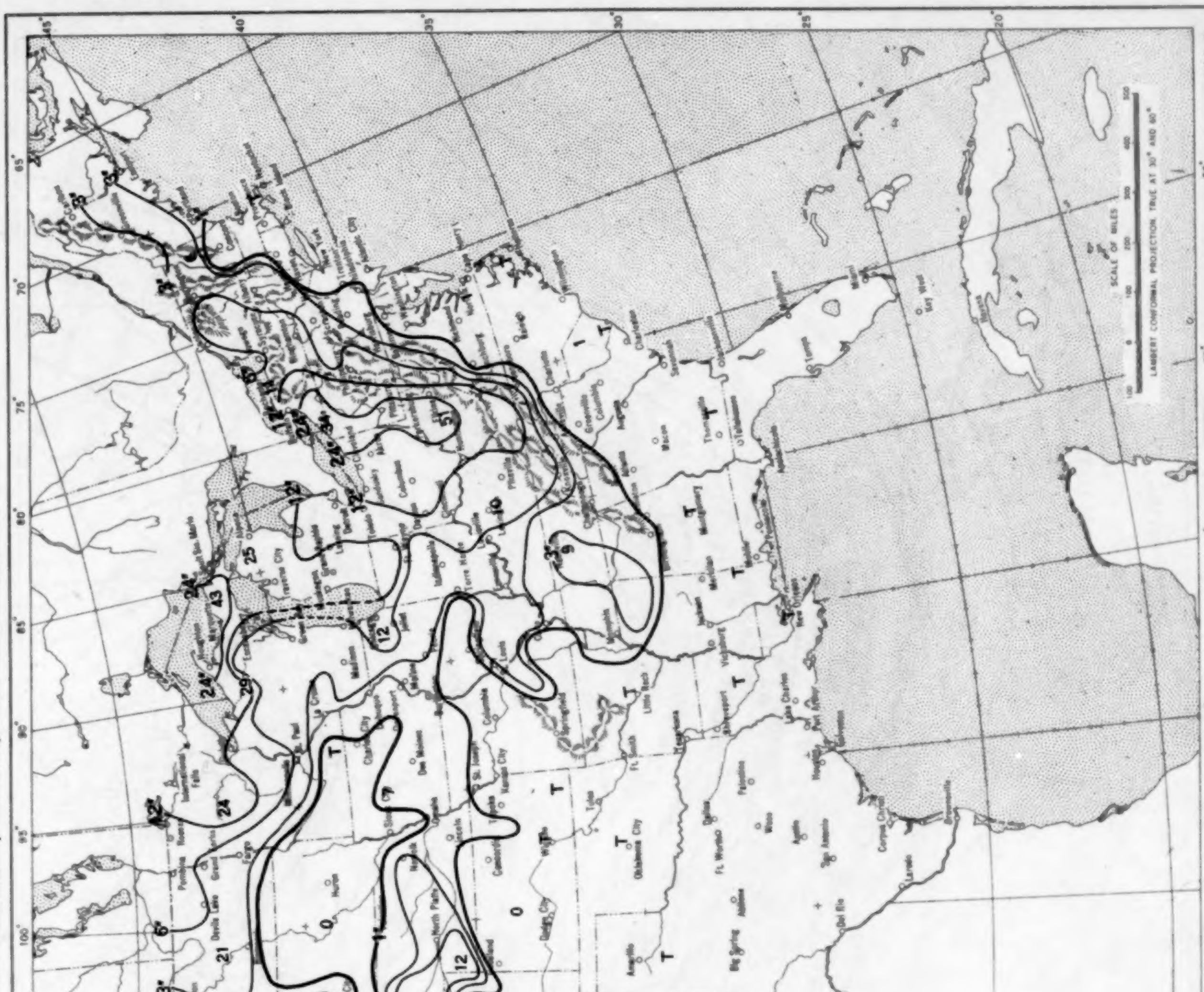

Chart VIII, November 1950. Contour Lines of Mean Dynamic Height (Geopotential) in Units of 0.98 Dynamic Meters and Mean Isotherms in Degrees Centigrade for the 850-millibar Pressure Surface, and Resultant Winds at 1,500 Meters (m. s. l.)

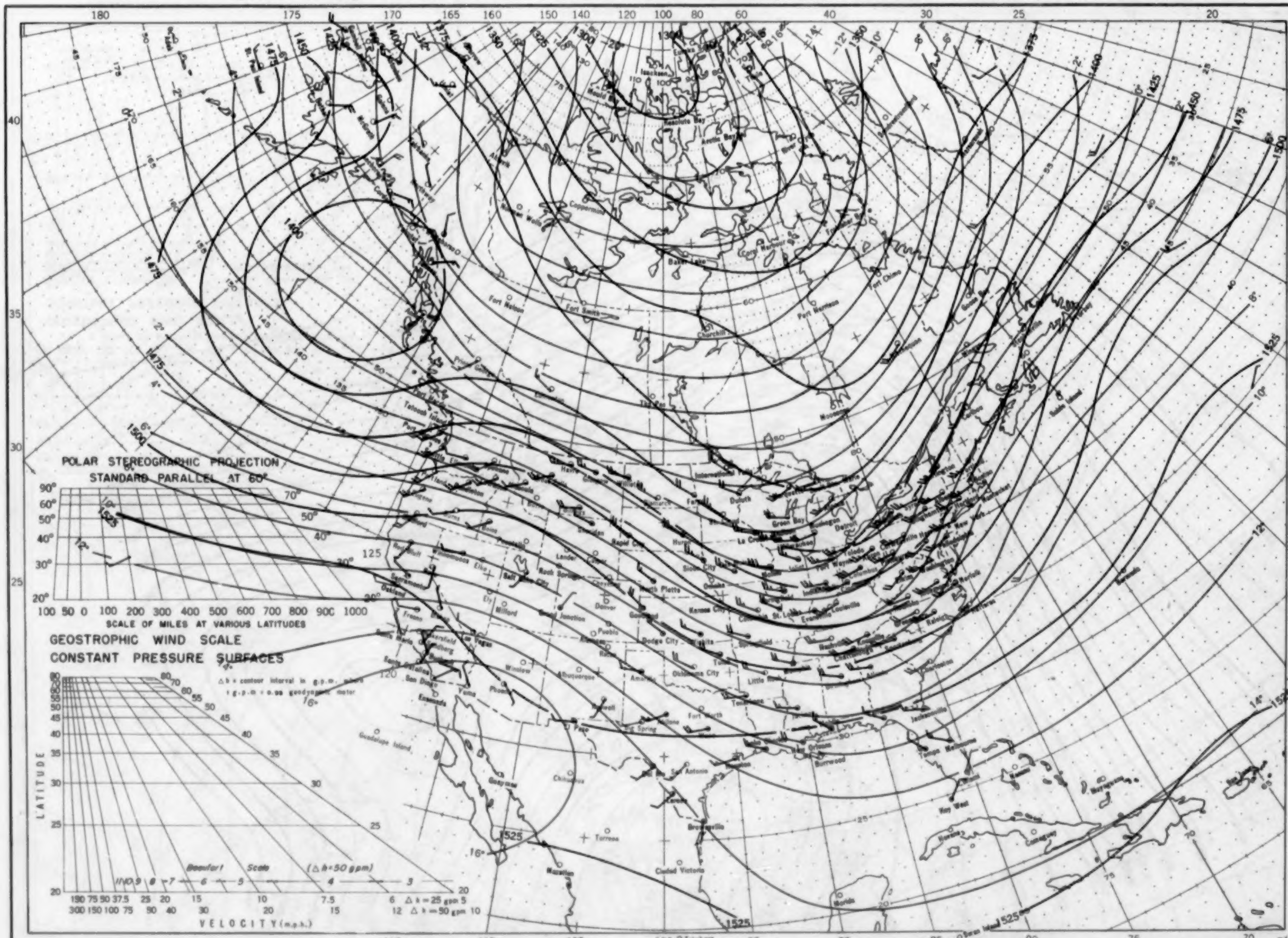

Contour lines and isotherms based on radiosonde observations at 0300 G. C. T. Winds indicated by black arrows based on pilot balloon observations at 2100 G. C. T.; those indicated by red arrows based on rawins taken at 0300 G. C. T.

Chart IX, November 1950. Contour Lines of Mean Dynamic Height (Geopotential) in Units of 0.98 Dynamic Meters and Mean Isotherms in Degrees Centigrade for the 700-millibar Pressure Surface, and Resultant Winds at 3,000 Meters (m. s. l.)

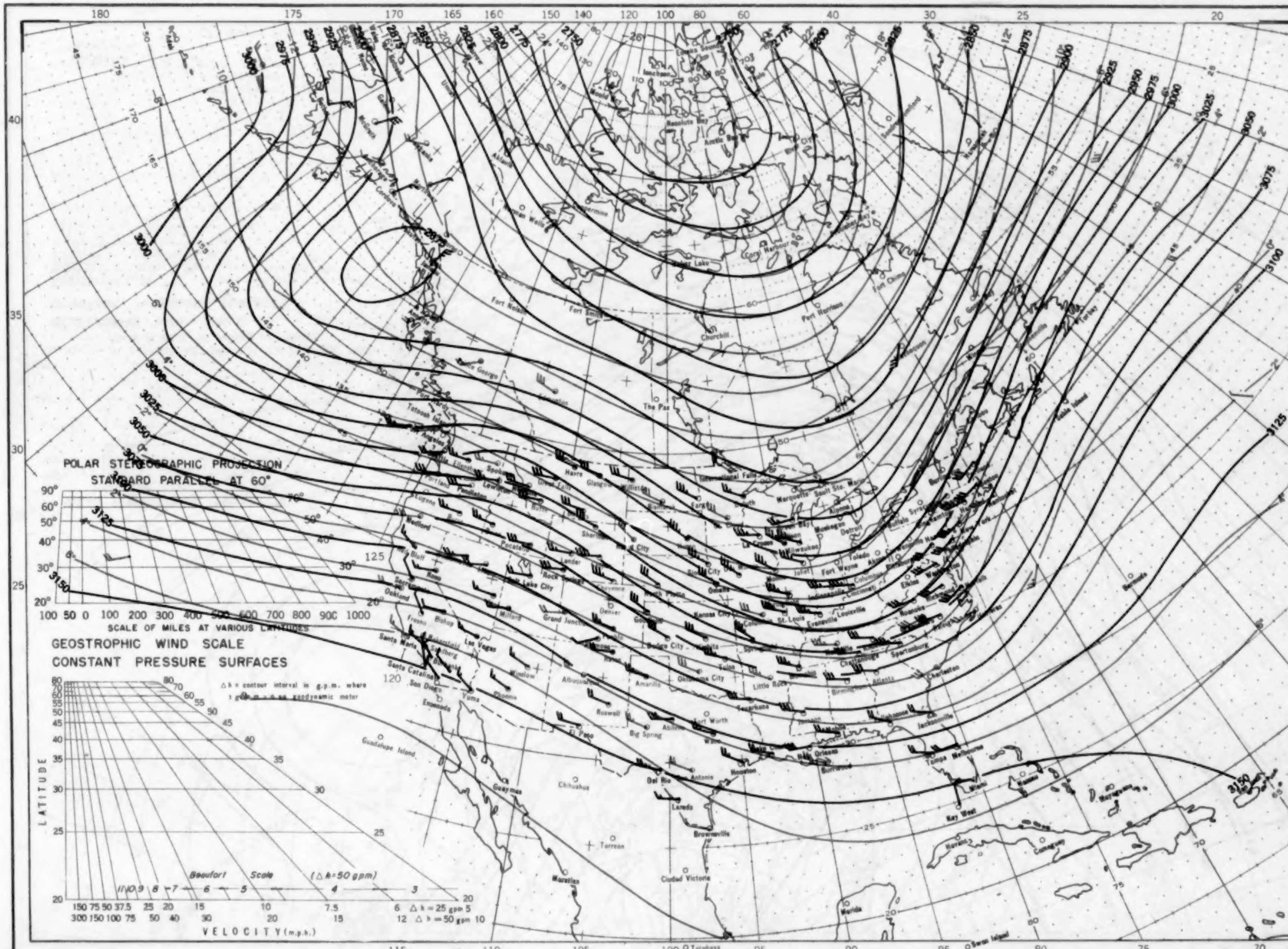

Contour lines and isotherms based on radiosonde observations at 0300 G. C. T. Winds indicated by black arrows based on pilot balloon observations at 2100 G. C. T.; those indicated by red arrows based on rawins taken at 0300 G. C. T.

Chart X, November 1950. Contour Lines of Mean Dynamic Height (Geopotential) in Units of 0.98 Dynamic Meters and Mean Isotherms in Degrees Centigrade for the 500-millibar Pressure Surface, and Resultant Winds at 5,000 Meters (m. s. l.)

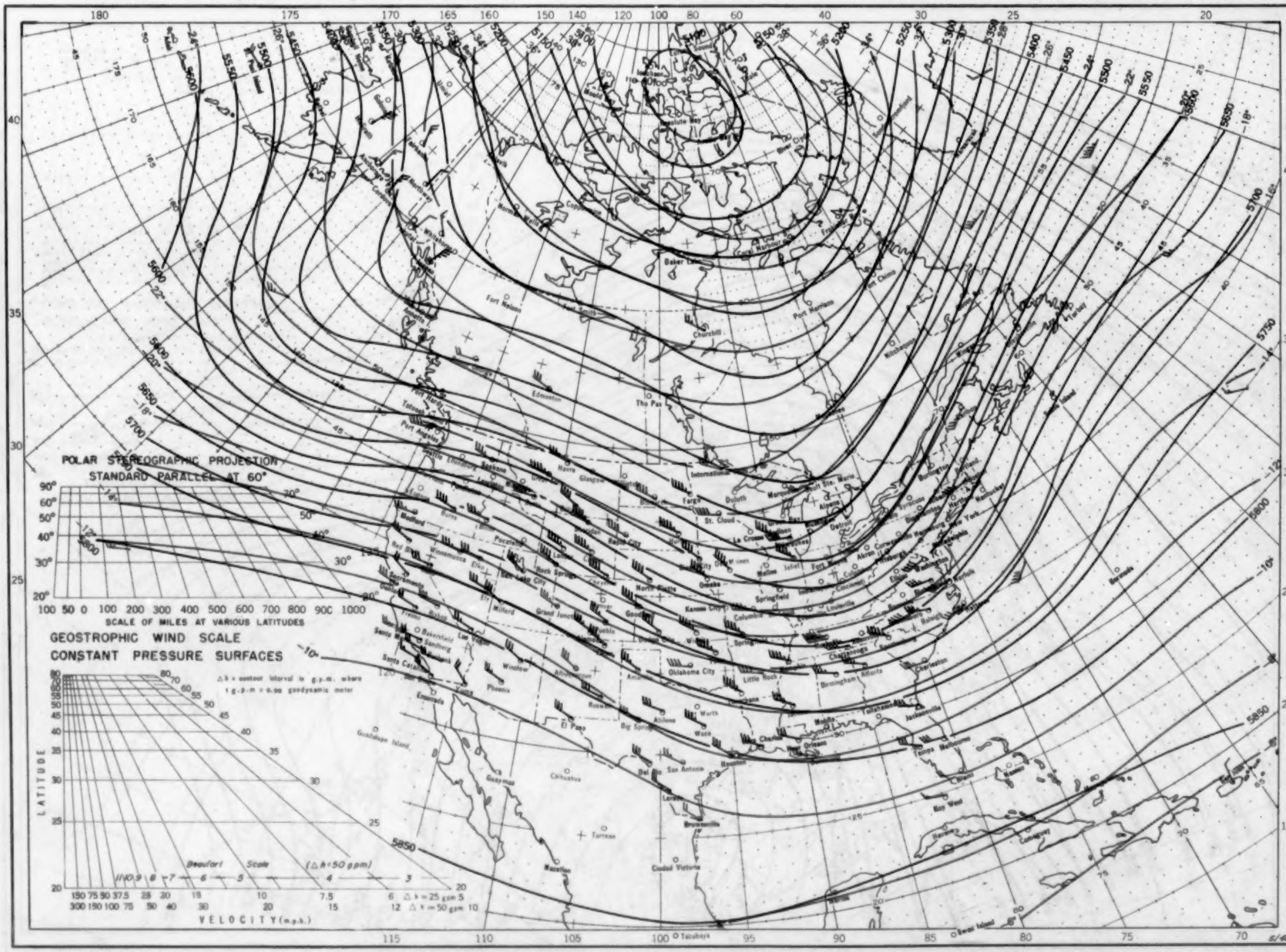

Contour lines and isotherms based on radiosonde observations at 0300 G. C. T. Winds indicated by black arrows based on pilot balloon observations at 2100 G. C. T.; those indicated by red arrows based on rawins taken at 0300 G. C. T.

Chart XI, November 1950. Contour Lines of Mean Dynamic Height (Geopotential) in Units of 0.98 Dynamic Meters and Mean Isotherms in Degrees Centigrade for the 300-millibar Pressure Surface, and Resultant Winds at 10,000 Meters (m. s. l.)

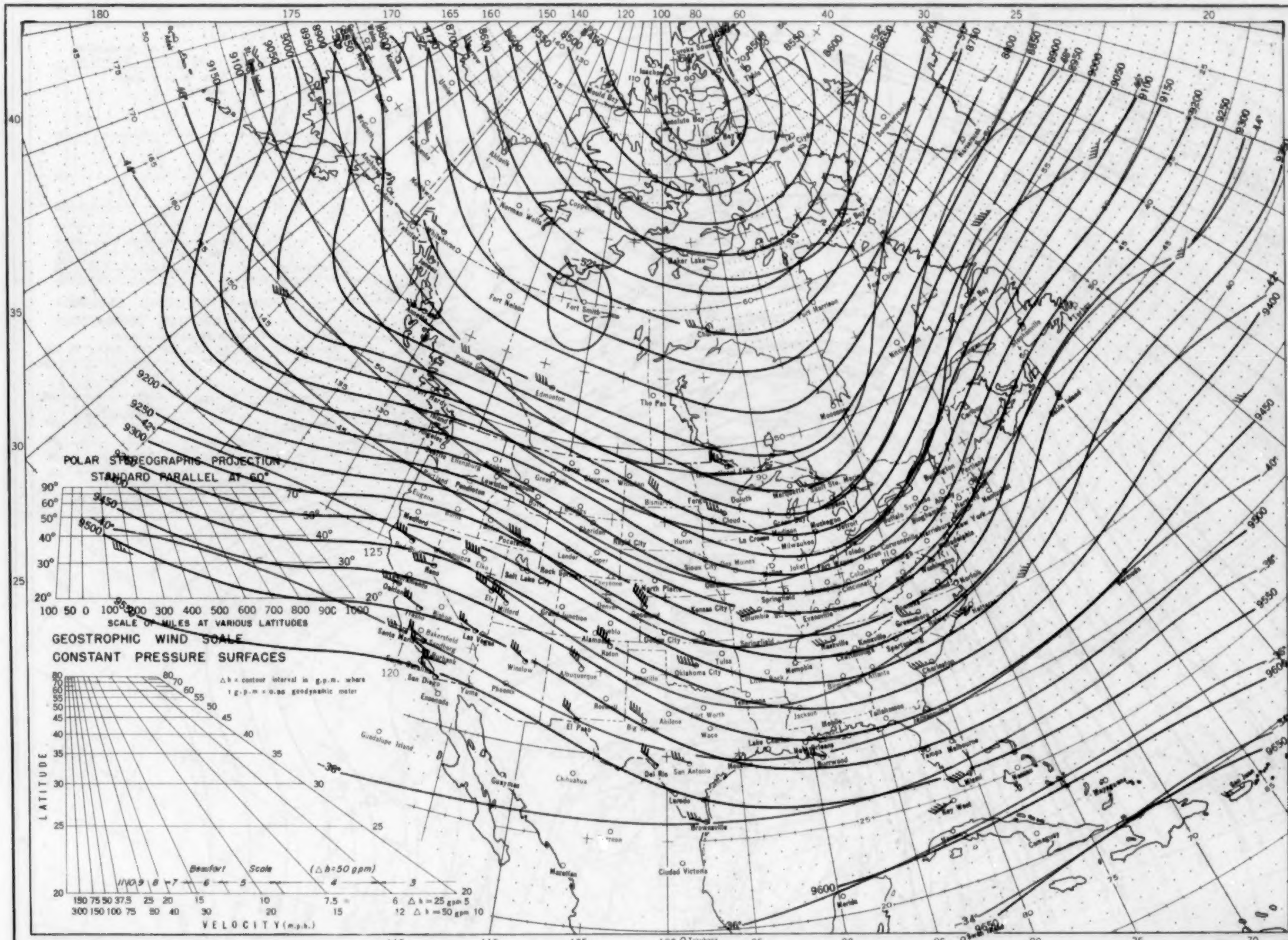

Contour lines and isotherms based on radiosonde observations at 0300 G. C. T. Winds indicated by black arrows based on pilot balloon observations at 2100 G. C. T.; those indicated by red arrows based on rawins taken at 0300 G. C. T.